UNIVERSITY OF JYVÄSKYLÄ

MASTER'S THESIS

Plasma cell-free DNA in diagnostic *KRAS* mutation testing

Aleksi Isomursu
University of Jyväskylä
Faculty of Mathematics and Science
Department of Biological and Environmental Science
Cell and Molecular Biology
06.01.2015

PREFACE

Abstract:

Anti-epidermal growth factor receptor (EGFR) monoclonal antibodies (mAb) are used for treating metastatic colorectal cancer (mCRC). Activating mutations in oncogenes *KRAS* and *NRAS* result in resistance to anti-EGFR mAbs, necessitating tumor genotyping prior to the therapy. However, tissue biopsy is an invasive procedure that may fail to address the spatiotemporal clonal heterogeneity of cancer. Circulating cell-free DNA (cfDNA) has been shown to contain oncogenic mutations originating from malignant cells, presenting a promising alternative source of tumor-derived genetic material.

We used temperature gradients and dilution series to develop and optimize an enhanced, improved and complete enrichment co-amplification at lower denaturation temperature PCR (E-ice-COLD-PCR) assay for the selective amplification of *KRAS* codon 12 and 13 mutations in plasma cfDNA; together these mutants comprise approximately 80% of all RAS mutations in colorectal cancer. The amplified variants were detected by subjecting the PCR products to allele quantification by targeted pyrosequencing. 16 mCRC patients were recruited and 4x3 ml of peripheral blood was drawn from each patient into K_2EDTA tubes. To evaluate the effect of centrifugation on cfDNA extraction and subsequent mutation testing, plasma was separated according to four different centrifugation protocols: 10 min at 500 x g; 10 min at 500 x g + 10 min at 16,000 x g; 10 min at 1,600 x g; and 10 min at 1,600 x g + 10 min at 16,000 x g. cfDNA was extracted from the plasma using commercially available silica membrane columns and the sample set displaying the least amount of genomic DNA contaminants was tested for *KRAS* codon 12 and 13 mutations. The results were compared to previously detected mutations in the patients' tumors.

The maximum analytical sensitivity for calling *KRAS* mutations c.35G>A and c.35G>C was 0.1% and 0.25% mutant in a wild type background, respectively, while the diagnostic limit of detection (LOD) was 0.25%-0.5% (α = 0.05). Concordant with previous studies, the average amount of cfDNA in the patients' blood was 59 ± 50 ng/ml ($\bar{x} \pm sd$). Concentrations varied according to the individual centrifugation protocol (P = 0.022). More specifically, plasma centrifuged for 10 min at 500 x g tended to yield slightly less cfDNA than any of the correlated samples, although the pairwise post-hoc comparisons did not reach statistical significance. When the samples were tested for *KRAS* mutations, the resulting sensitivity was 17% and the specificity 89%.

E-ice-COLD-PCR-enhanced targeted pyrosequencing allows for robust and sensitive detection of *KRAS* c.35G>A and c.35G>C from minute amounts of DNA. Even though the test performance was not directly validated for other hotspot mutations in *KRAS* codons 12 and 13 (i.e. c.34G>T, c.34G>A, c.34G>C, c.35G>T and c.38G>A), this can be accomplished separately as needed. The method can be used for detecting pathogenic *KRAS* mutations in the cfDNA of mCRC patients. This may prove useful for tumor genotyping when conventional tissue samples are unavailable or repeated testing is required, e.g. in the early detection of acquired resistance. However, due to the observed sensitivity issues, comprehensive prospective studies are needed to confirm the viability of the test for clinical use.

Tiivistelmä:

Epidermaalisen kasvutekijän reseptorin (EGFR) monoklonaalisia vasta-aineita (mAb) käytetään apuna metastaattisen kolorektaalisyövän (mCRC) hoidossa. Aktivoivat mutaatiot *KRAS*- ja *NRAS*-onkogeeneissä tekevät syöpäsolut vastustuskykyisiksi anti-EGFR-vasta-aineille, ja tästä syystä tuumorit tulee genotyypittää ennen hoidon aloittamista. Kudosbiopsian ottaminen on kuitenkin invasiivinen toimenpide, eikä näyte välttämättä edusta kattavasti syövän kaikkien solupopulaatioiden geneettisiä muutoksia. Verenkierron solunulkoisen DNA:n (cfDNA) on havaittu sisältävän maligneista soluista lähtöisin olevia onkogeenisiä mutaatioita, ja se voi olla hyvä vaihtoehtoinen tuumoriperäisen DNA:n lähde.

Kehitimme ja optimoimme lämpötilagradienttien ja laimennossarjojen avulla E-ice-COLD-PCR (engl. *enhanced, improved and complete enrichment co-amplification at lower denaturation temperature PCR*)-pohjaisen menetelmän plasman cfDNA:ssa esiintyvien *KRAS*-geenin kodonien 12 ja 13 mutaatioiden selektiiviseen monistamiseen; nämä mutantit vastaavat yhdessä noin 80 %:a kolorektaalisyövän kaikista RAS-mutaatioista. Monistetut mutantit osoitettiin mittaamalla PCR-tuotteista löytyvien alleelien määrät kohdennetun pyrosekvensoinnin avulla. 16:sta mCRC-potilaasta kerättiin 4x3 ml perifeeristä verta K_2EDTA-putkiin. Sentrifugoinnin vaikutusta cfDNA:n eristämiseen ja sen jälkeiseen mutaatiomääritykseen arvioitiin erottelemalla plasma soluista neljän erilaisen sentrifugointiprotokollan mukaan: 10 min/500 x g; 10 min/500 x g + 10 min/16000 x g; 10 min/1600 x g; sekä 10 min/1600 x g + 10 min/16000 x g. cfDNA eristettiin plasmasta kaupallisilla piidioksidikalvopylväillä, ja näytteet joissa havaittiin vähiten kontaminoivaa genomista DNA:ta valittiin *KRAS*-mutaatiomääritykseen. Tuloksia verrattiin potilaiden tautimuutoksista aiemmin osoitettuihin mutaatioihin.

Testin analyyttinen herkkyys *KRAS*-mutaatioita osoitettaessa oli 0,1 % (c.35G>A)-0,25 % (c.35G>C). Diagnostinen havaitsemisraja (LOD) oli vastaavasti 0,25 %-0,5 % ($\alpha = 0,05$). cfDNA:ta oli potilaiden veressä keskimäärin 59 ± 50 ng/ml ($\bar{x} \pm sd$), ja tulokset vastasivat tältä osin aiemmin julkaistuja tutkimuksia. Konsentraatio vaihteli sentrifugointiprotokollan mukaan (P = 0,022): 10 min 500 x g:llä erotellusta plasmasta eristettiin yleisesti ottaen hieman vähemmän cfDNA:ta kuin saman potilaan muista näytteistä. Kahdenvälisissä post-hoc-analyyseissä havaitut erot eivät kuitenkaan olleet tilastollisesti merkitseviä. Kun näytteistä määritettiin *KRAS*-mutaatioita, menetelmän herkkyys oli 17 % ja spesifisyys 89 %.

E-ice-COLD-PCR-avusteinen kohdennettu pyrosekvensointi mahdollistaa *KRAS*-mutaatioiden c.35G>A ja c.35G>C herkän havaitsemisen pienestäkin määrästä DNA:ta. Vaikka testin tarkkaa suorituskykyä ei määritetty erikseen muilla *KRAS*-geenin kodoneissa 12 ja 13 esiintyvillä mutaatioilla (c.34G>T, c.34G>A, c.34G>C, c.35G>T ja c.38G>A), tämä on tarvittaessa helposti toteutettavissa. Testillä voidaan havaita patogeenisiä *KRAS*-mutaatioita myös mCRC-potilaiden cfDNA:sta, mistä voi olla hyötyä kun tavanomaisia kudosnäytteitä ei ole saatavilla tai kun halutaan suorittaa useita perättäisiä mutaatiomäärityksiä, esimerkiksi hankinnaisen resistenssin havaitsemiseksi. Diagnostisessa herkkyydessä todettujen puutteiden vuoksi testin kliininen validointi edellyttää kuitenkin kattavia, prospektiivisia jatkotutkimuksia.

Avainsanat: metastaattinen kolorektaalisyöpä, yksilöllistetty hoito, *KRAS*-geenin mutaatiomääritys, E-ice-COLD-PCR, pyrosekvensointi

TABLE OF CONTENTS

ABBREVIATIONS

cfDNA	cell-free DNA
ctDNA	circulating tumor DNA
E-ice-COLD-PCR	enhanced, improved and complete enrichment co-amplification at lower denaturation temperature PCR
EGFR	epidermal growth factor receptor
ERK	extracellular signal-regulated kinase
LNA	locked nucleic acid
LOB	limit of blank
LOD	limit of detection
mAb	monoclonal antibody
mCRC	metastatic colorectal cancer
Raf	rapidly accelerated fibrosarcoma
Ras	rat sarcoma
RS	reference strand
T_c	critical temperature

1 INTRODUCTION

1.1 Molecularly targeted cancer therapies

Despite the work of numerous researchers and physicians, cancer remains a major cause of death and morbidity worldwide. In Europe alone, cancer kills an estimated 1.75 million people annually (Ferlay et al., 2013). The four most common cancer sites, breast cancer, colorectal cancer, prostate cancer and lung cancer, constitute approximately one half of the total European cancer burden. Finland is not an exception: in 2012, 137.9 Finnish males and 123.5 females out of every 100,000 were diagnosed with one of these types of cancer (Adjusted for age; Finnish Cancer Registry, 2014).

Although the average prognosis for cancer patients has improved during the 20th century, some of this progress can be attributed to better diagnostic methods and routine screening programs (Malmgren et al., 2012; Shaukat et al., 2013). Cancer treatments with curative intent, such as radical surgery combined with adjuvant radiation and/or chemotherapy, or radical chemoradiotherapy often fail in locally advanced or metastatic diseases (Reviewed by Batista et al., 2013; Chermiti Ben Abdallah et al., 2014; Damin and Lazzaron, 2014). Indeed, advanced cancers are often inoperable, in which case the treatment depends entirely on pharmacological agents and radiotherapy.

The past decades have seen a considerable increase in our understanding of the biology of cancer, including its metabolism and signaling pathways (Reviewed by Hanahan and Weinberg, 2011). As the genetic and biochemical bases of carcinogenesis are being elucidated, the idea of targeting these same mechanisms for treatment is also becoming more and more relevant. Molecularly targeted therapies aim to destroy the malignant cells selectively, displaying decreased or no activity against healthy tissues (Reviewed by Huang et al., 2014). Ideally, this improves treatment efficacy while simultaneously reducing the drug's toxicity and harmful side effects. The goal of tailoring treatments to optimally benefit each individual patient makes modern cancer medicine a type of personalized medicine.

One of the most striking features of cancer is its high adaptability. An elevated rate of mutagenesis and various epigenetic alterations help the disease overcome different intra- and intercellular safety mechanisms that usually prevent cells from turning malignant. Six traditional hallmarks associated with virtually all types of cancer include sustained proliferative signaling, evasion of growth suppression, activation of invasion and metastasis, replicative immortality (i.e. avoiding quiescence induced by continuous mitoses), enhanced angiogenesis and resistance to apoptotic signals. Recently this list has been complemented by two new putative hallmarks: the ability to avoid destruction by the host's immune system and deregulation of energy metabolism, including the implementation of aerobic glycolysis (Hanahan and Weinberg, 2011).

To date, studies have identified approximately 140 genes that can be mutated to promote carcinogenesis and enable cells to express the hallmarks of cancer; such genes have been aptly named driver genes (Reviewed by Vogelstein et al., 2013). Driver genes can be further classified into oncogenes (promote cancer development when overexpressed or otherwise aberrantly active) and tumor suppressor genes (wild type suppressors inhibit tumorigenesis, for example by contributing to DNA repair mechanisms). Even though this diversity might seem exhausting when planning a therapeutic intervention, individual cancers typically present with only a few discrete driver mutations (Kandoth et al., 2013; Vogelstein et al., 2013). Moreover, every driver mutation known so far affects one or more of twelve intracellular signaling pathways that grant the malignant cells a selective growth advantage over their benign counterparts (Vogelstein et al., 2013). Among these, one of the best characterized is the extracellular signal-regulated kinase (ERK) pathway.

1.2 Extracellular signal-regulated kinase pathway

The ERK pathway (Fig. 1) is one of the four mammalian mitogen-activated protein kinase pathways. These pathways are involved in the regulation of cell survival, proliferation, differentiation and more. Whereas most of them will react readily to environmental stress, such as ionizing radiation, the ERK pathway is activated exclusively by extracellular growth factors (Reviewed by Roberts and Der, 2007). One of the major regulators of the ERK pathway is the ErbB family transmembrane tyrosine kinase known as epidermal growth factor

receptor (EGFR). Ligands like epidermal growth factor, transforming growth factor alpha and epiregulin bind EGFR, leading to its dimerization and subsequent activation. EGFR then recruits adaptor proteins SHC-transforming protein 1 and growth factor receptor-bound protein 2 (Basu et al., 1994), which in turn bind the guanine nucleotide exchange factor son of sevenless. Son of sevenless activates rat sarcoma (Ras) GTPases (K-Ras, N-Ras and H-Ras), and these small G-proteins bind and activate rapidly accelerated fibrosarcoma (Raf) kinases (A-Raf, B-Raf, and c-Raf-1). Raf kinases activate mitogen-activated protein kinase kinases 1 and 2, which phosphorylate and activate the two isoforms of ERK (ERK1/2) (Roberts and Der, 2007).
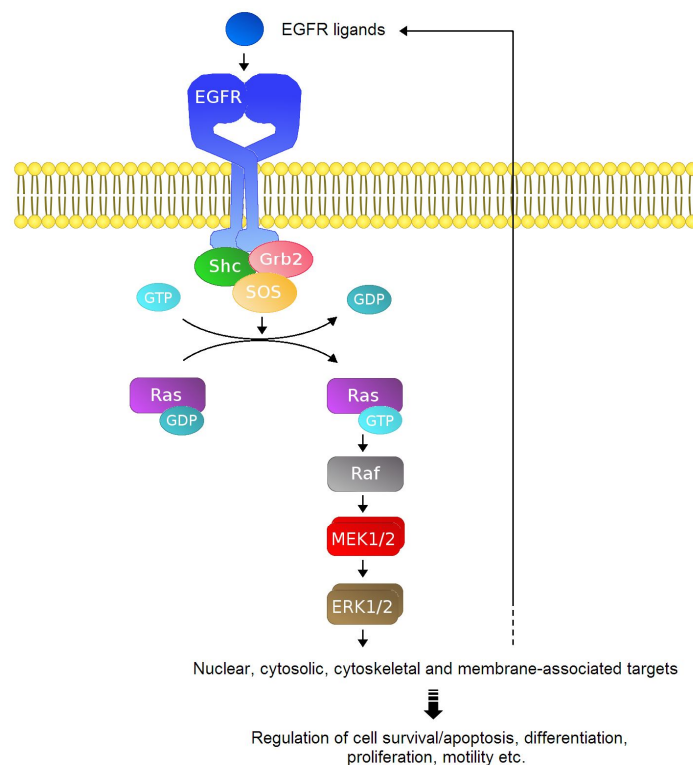
Figure 1. Schematic representation of the ERK pathway. Often depicted as simple linear cascades, all the different mitogen-activated protein kinase pathways exhibit extensive crosstalk with each other and several additional signaling pathways. EGFR, Ras proteins and ERK1/2 all alter cellular functions through a number of different effector molecules, and this complexity presents a challenge for researchers studying the ERK pathway as a putative target for cancer therapeutics. The figure is based on Basu et al. (1994), Roberts and Der (2007), Schulze et al. (2001) and Wortzel and Seger (2011).

While the Raf kinases and mitogen-activated protein kinase kinases 1 and 2 have very restricted substrate specificities, ERK1/2 can interact with approximately 200 different effector molecules (Reviewed by Wortzel and Seger, 2011). These effectors include cytoskeletal elements, regulators of apoptosis, a large number of different transcription factors and more. Signaling specificity is adjusted by additional factors, e.g. the sub-cellular localization of the ERK cascade components, interactions with scaffold proteins, crosstalk with other signaling pathways and the duration and strength of the signal itself (Roberts and Der, 2007; Wortzel and Seger, 2011). Activation of ERK1/2 upregulates the expression of EGFR ligands, resulting in an autocrine feedback mechanism that promotes signaling through the ERK pathway (Schulze et al., 2001).

Activating mutations in genes coding for the ERK pathway components are some of the most common genetic alterations found in cancer. For example, the gene *EGFR* is mutated in approximately 10% of lung adenocarcinomas and over 25% of all glioblastomas (Kandoth et al., 2013), while activating mutations in *BRAF*, the gene coding for B-Raf, are found in approximately 50% of malignant melanomas (reviewed by Ascierto et al., 2012). *KRAS* (i.e. Kirsten rat sarcoma viral oncogene homolog), *NRAS* (i.e. neuroblastoma RAS viral (v-ras) oncogene homolog) and *HRAS* (i.e. Harvey rat sarcoma viral oncogene homolog), collectively known as the RAS oncogenes, are some of the most thoroughly studied human oncogenes. The genes code for K-Ras, N-Ras and H-Ras, respectively. While the frequency of RAS mutations across all cancer types has been traditionally reported to be as high as 30% (Fernández-Medarde and Santos, 2011), this value is probably distorted due to a screening bias: colorectal cancer dominates the analyzed data, and the correct pan-cancer frequency of all RAS mutations is likely closer to 15% (Prior et al., 2012). Considerable variation between the different RAS genes and cancer types exists: for example, *KRAS* is mutated in at least 60% of pancreatic cancers, whereas the rate of *NRAS* and *HRAS* mutations in such tumors is 1-2% at best (Fernández-Medarde and Santos, 2011; Prior et al., 2012).

1.3 Colorectal cancer and diagnostic RAS mutation testing

Due to the high prevalence of cancer-associated ERK pathway mutations and the biological rationale supporting their role in oncogenesis, the ERK cascade components have been prime candidates for cancer drug discovery (Reviewed by Montagut and Settleman, 2009; Roberts and Der, 2007). EGFR inhibitors, in particular, are a class of targeted therapeutics that has been successfully utilized in the treatment of several different cancer types. They comprise both anti-EGFR monoclonal antibodies (mAb) (e.g. cetuximab, panitumumab) and small molecule tyrosine kinase inhibitors (e.g. gefitinib, erlotinib). Anti-EGFR mAbs bind the extracellular domains of EGFR molecules, preventing ligand-receptor interactions and recruiting natural killer cells to destroy the EGFR-expressing cells (Oppenheim et al., 2014). Kinase inhibitors bind the receptors' intracellular kinase domains, hampering their ability to recruit ATP (Roberts and Der, 2007).

In combination with conventional chemotherapeutic agents, cetuximab and panitumumab are indicated for treatment of metastatic colorectal cancer (mCRC) (Erbitux® SmPC; Vectibix® SmPC). Initial trials with the mAbs produced mixed results, as only a small sub-population of EGFR-expressing tumors responded to the treatment and a slightly larger fraction of the study population presented with a stable disease (Cunningham et al., 2004; Saltz et al., 2004). Eventually CRYSTAL (Van Cutsem et al., 2009), PRIME (Douillard et al., 2010) and OPUS (Bokemeyer et al., 2011) studies recognized the mutation status of *KRAS* exon two as a predictive biomarker for response to anti-EGFR mAbs. Acting downstream of EGFR, mutated *KRAS* and its aberrantly active gene product promote signaling through the ERK pathway regardless of EGFR status. Moreover, treating *KRAS* mutation positive tumors with mAbs leads to an increased risk of disease progression compared to the standard FOLFOX treatment (a chemotherapy regimen consisting of folinic acid, fluorouracil and oxaliplatin) (Bokemeyer et al., 2011). The same adverse effect was later observed in patients whose tumors harbored activating mutations in *KRAS* exons three or four, as well as those with mutations in *NRAS* exons two, three or four (Douillard et al., 2013). On the other hand, *HRAS* mutations occur in colorectal cancer very infrequently and their role in the pathogenicity of mCRC seems to be negligible.

Even though the activating effect of *KRAS* codon 13 (located in exon two) mutations has occasionally been disputed (De Roock et al., 2010), the use of Vectibix® (panitumumab) is currently limited to patients whose tumors have been genotyped and recognized as wild type in regards to *KRAS* and *NRAS* exons two, three and four (Vectibix® SmPC). Indeed, approximately 50% of all colorectal cancers are RAS mutation positive (Fig. 2). Approximately 80% of the mutations reside in codons 12 and 13 of *KRAS* exon two (Douillard et al., 2013), with *KRAS* c.35G>A (p.G12D), c.35G>T (p.G12V) and c.38G>A (p.G13D) accounting for 13%, 10% and 8% of all RAS mutations, respectively (Vaughn et al., 2011). The reason behind the relative abundance of certain base alterations is not clear, although genetic, epigenetic and protein based mechanisms have been proposed (Prior et al., 2012). In particular, despite being structurally almost identical, *KRAS* and *NRAS* are not functionally redundant. Partially distinct roles in intracellular signaling may account for the frequency at which each mutant isoform is observed in a particular cancer type.
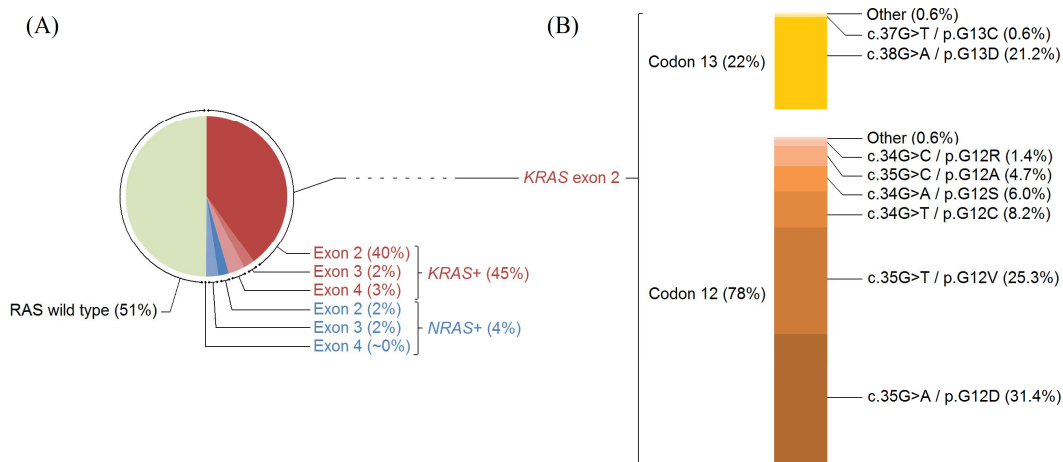
Figure 2. RAS mutations in colorectal cancer. The list is not exhaustive, as some very rare variants of unknown pathogenicity have been excluded. (A) Relative frequencies at which the different exons of *KRAS* and *NRAS* are mutated. Based on Douillard et al. (2013). (B) Distribution of activating mutations within *KRAS* exon two. Based on Vaughn et al. (2011).

Diagnostic mutation testing is typically conducted using DNA from formalin fixed, paraffin embedded tissue specimen. While this approach may work well technically, in a clinical setting it has several notable drawbacks: a tissue sample may be too small, otherwise ill-suited for tumor genotyping (e.g. a vast majority of cells might be necrotic or benign) or simply

unavailable. Taking a biopsy is a time-consuming process that carries a risk of complications to the patient. Partly for this reason, repeated sampling during the course of a treatment is rare.

Studying DNA from a single biopsy may fail to address the spatiotemporal clonal heterogeneity of cancer. Virtually every cancer presents with high inter- and intratumoral clonal heterogeneity, i.e. they consist of several genetically distinct sub-populations of malignant cells (Gerlinger et al., 2012). Moreover, the rapidly mutating cancers tend to become resistant to the therapeutic agents that are being used to treat them. In the case of EGFR inhibitors, acquired resistance often arises due to somatic activating mutations in the ERK pathway genes, *KRAS* in particular (Bettegowda et al., 2014; Misale et al., 2012). By analyzing only samples that were taken during the initiation of the treatment, physicians are unable to predict or verify the development of acquired resistance mechanisms and cannot respond by changing the treatment regimen that has now lost effectiveness and become merely toxic to the patient.

1.4 Circulating cell-free DNA and cancer

Cell-free DNA (cfDNA) comprises all extracellular DNA present in a given body. Circulating cfDNA was first discovered in 1948 (Mandel and Metais, 1948), and a link between cfDNA and cancer was established less than 20 years later when Bendich et al. (1965) proposed that circulating nucleic acids may promote oncogenesis. Today, cfDNA is a valuable diagnostic tool used in fetal mutation testing and more (Macher et al., 2012). It is also one of the most promising new candidates for a novel cancer biomarker (reviewed by Diaz Jr and Bardelli, 2014).

Healthy individuals have only minute amounts of cfDNA in their blood, usually in the order of a few nanograms per milliliter. The concentration is increased in cancer, however, and patients with advanced disease can have blood cfDNA concentrations of 100-1000 ng/ml or more (Jahr et al., 2001; Park et al., 2012; Sozzi et al., 2001). Considerable variation in the yields can be observed, some of which originates from the current differences in methods and reporting between research groups (reviewed by Jung et al., 2010).

cfDNA that originates exclusively from malignant cells is called circulating tumor DNA (ctDNA). Typically, it comprises only a small fraction of the total blood cfDNA (0.01-10%) (Diaz Jr and Bardelli, 2014; Diehl et al., 2005; Diehl et al., 2008), although frequencies of approximately 90% have also been reported (Jahr et al., 2001). Absolute and relative ctDNA concentrations, as well as the prevalence of cancer patients who have detectable levels of ctDNA in their blood, are all strongly correlated to cancer type (Bettegowda et al., 2014) and clinicopathological features such as tumor stage (Bettegowda et al., 2014; Diehl et al., 2005). For example, a vast majority of mCRC patients (95% CI: 86-100%) present with detectable ctDNA concentrations (Bettegowda et al., 2014), and ctDNA harboring oncogenic mutations may comprise as much as 1.9-27% of their total circulating cfDNA (Diehl et al., 2005).

Several mechanisms for cfDNA release have been proposed (Fig. 3). For example, the lysis of hematopoietic cells (Lui et al., 2002a) and active release by various cell types (Reviewed by Peters and Pretorius, 2011; Rak, 2013) have both been postulated to contribute to the total circulating cfDNA. Furthermore, the growth of an aggressive tumor can cause hypoxia, which in turn promotes significant necrosis and/or apoptosis of malignant cells and surrounding tissues. The debris from dying cells is normally phagocytosed and removed by macrophages. It is not clear whether this process is hampered in cancerous tissues (Jahr et al., 2001) or if the macrophages actually return some of the necrotic DNA back to circulation, as proposed by Diehl et al. (2005). Circulating cfDNA is often associated with extracellular vesicles or other molecules, such as histones, which shield the nucleic acids from enzymatic degradation (Peters and Pretorius, 2011).

Somatic mutations and epigenetic alterations found in a tumor can serve as personalized biomarkers that allow the observation and quantification of ctDNA separately from the rest of the cfDNA. In particular, quantitative analyses of ctDNA may be used for monitoring disease progression (Diehl et al., 2008; Dawson et al., 2013). Other potential applications of ctDNA-based testing include early detection of residual disease (Diehl et al., 2008) or acquired resistance to therapeutics (Misale et al., 2012). In these cases, oncogenic mutations found in the patient's blood may serve as an early warning sign before any clinical symptoms can be detected.
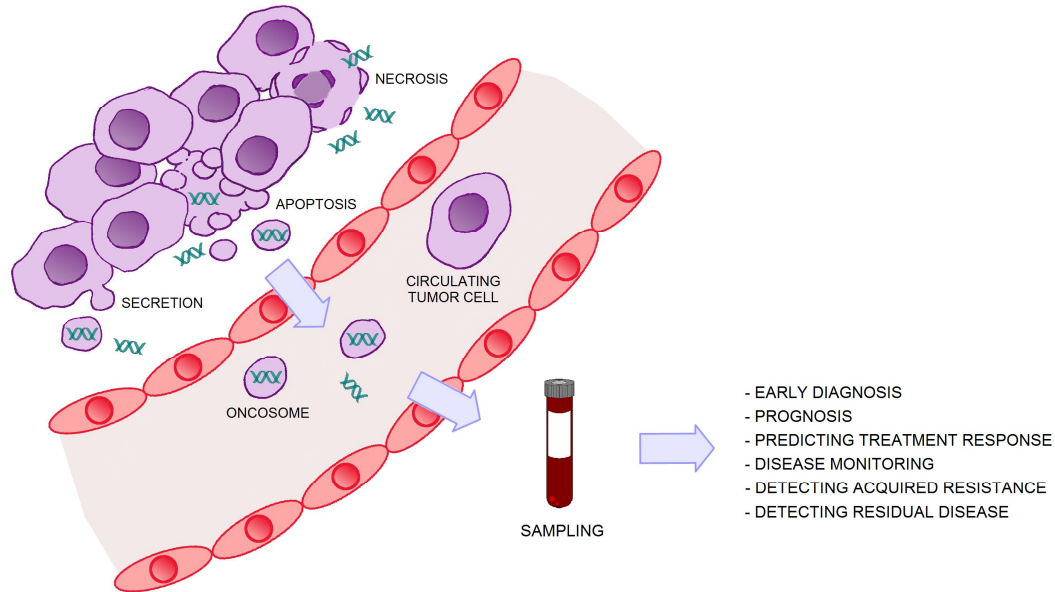
Figure 3. ctDNA and liquid biopsy. Malignant cells, whether viable or dying, release fragmented DNA that ends up in circulation. Some of the circulating nucleic acids are associated with other molecules or different extracellular vesicles; such oncogene-containing vesicles are known collectively as oncosomes. Furthermore, the blood of a cancer patient often contains circulating tumor cells. These are relatively rare and their contribution to the total ctDNA is low at best. However, the cells themselves may often be used as a prognostic biomarker. After venipuncture and DNA extraction, ctDNA can be analyzed to answer a number of different diagnostic questions. The figure is based on Bettegowda et al. (2014), Diaz Jr and Bardelli (2014), and Rak (2013).

Genotyping malignant cells by analyzing ctDNA is also possible, and specific mutations may often have direct treatment implications. This is also the case with the ERK pathway genes and EGFR inhibitors, and indeed, *KRAS*, *EGFR* and *BRAF* have all been genotyped using plasma as a source of ctDNA (Diehl et al., 2008; Pupilli et al., 2013 Taniguchi et al., 2011). Because these genetic analyses resemble those conducted from conventional tissue biopsies, ctDNA-based testing is also known as liquid biopsy.

From a diagnostic standpoint, liquid biopsy has several appealing qualities: venipuncture is a quick, easy and relatively non-invasive procedure, allowing for repeated sampling when needed. The half-life of circulating cfDNA is also short, estimated to be a few hours at most (Diehl et al., 2008; Lo et al., 1999; To et al., 2003), which makes tumor-derived ctDNA a useful tool for tracking the genetic changes that take place within an individual cancer. Moreover, by using the patient's blood as a source of ctDNA, the problem of clonal

heterogeneity may be addressed: ideally, DNA from all the different sub-populations of malignant cells in a body can be studied simultaneously (Chan et al., 2013).

The main constraint that limits the use of ctDNA in cancer diagnostics is its scarcity. As ctDNA concentrations are modest at best, any study or diagnostic procedure that aims to quantitate or genotype oncogenic mutations present in blood requires extremely sensitive testing methods. So far several techniques have yielded promising results: some examples are quantitative PCR (Pupilli et al., 2013), next generation sequencing (Bettegowda et al., 2014; Chan et al., 2013; Dawson et al., 2013), digital PCR and its derivatives (Dawson et al., 2013; Diehl et al., 2005; Diehl et al., 2008), high resolution melting analysis (Macher et al., 2012), digital karyotyping (Leary et al., 2012) and several PCR-based methods that selectively amplify and enrich different mutant alleles.

1.5 *Enhanced, improved and complete enrichment co-amplification at lower denaturation temperature PCR*

Enhanced, improved and complete enrichment co-amplification at lower denaturation temperature PCR (E-ice-COLD-PCR) is a novel PCR-based technique that selectively amplifies different low-frequency allele variants in a sample of DNA (How Kit et al., 2013). The original predecessor of E-ice-COLD-PCR, known simply as COLD-PCR, is a simple and straightforward method capable of enriching all known and unknown mutations within a selected amplicon (Li et al., 2008). However, the technique has a significant restriction as the operator must choose between excessively long reaction times coupled with low to moderate allele enrichment (full COLD-PCR) and a shorter, more efficient reaction that only enriches mutations that lower melting temperature, i.e. G/C → T/A and deletions (fast COLD-PCR).

In E-ice-COLD-PCR, additional reference strands (RS) are included in the reaction. These oligonucleotides are complementary to the wild type amplicon and may or may not overlap slightly with one of the two PCR primer binding sites. RSs are fitted with non-extensible 3' phosphate groups to prevent elongation by DNA polymerases, while locked nucleic acid (LNA) bases are included around the putative mutation sites for improved binding specificity (Owczarzy et al., 2011; You et al., 2006).

The reaction starts with multiple cycles of conventional PCR, followed by a denaturation step at 95 °C. As the sample cools down, both mutant and wild type strands bind to the more abundant RSs. However, the duplexes with a mismatch (mutant-RS) have significantly lower melting temperatures than their perfectly matched counterparts (wild type-RS). An additional denaturation step at a lower temperature (known as critical temperature or T_c) allows for selective melting and subsequent amplification of the mutant-RS duplexes (Fig. 4)
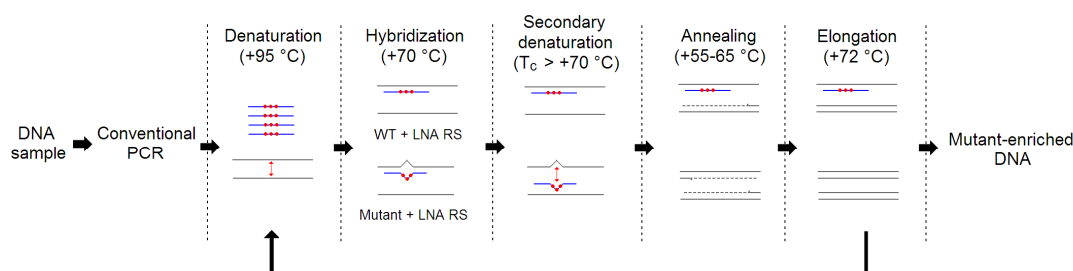
Figure 4. Working principle of E-ice-COLD-PCR. A large excess of RSs (blue strands) ensures efficient binding to both mutant and wild type strands, and consequently duplexes between two template strands are rare. LNA bases (red dots) increase binding specificity. As a result, even a single mismatch reduces the melting temperature of the heteroduplex significantly, allowing for robust enrichment of low-frequency alleles. The figure is based on How Kit et al. (2013).

E-ice-COLD-PCR combines the shorter reaction times and efficient mutation enrichment of fast COLD-PCR with full COLD-PCR's robustness and ability to amplify all mutation types. Unlike the early versions of COLD-PCR, E-ice-COLD-PCR tolerates changes in T_c very well and gradients of up to 10 °C have been shown to result in strong overall mutation enrichment (How Kit et al., 2013). However, in order to benefit from the inclusion of LNAs, the RSs must be designed with prior knowledge of putative mutation sites.

After E-ice-COLD-PCR, the PCR products are analyzed to detect and/or quantify the enriched mutant alleles. This can be accomplished by a number of different methods, including quantitative PCR, melting analysis, Sanger sequencing and pyrosequencing. Combined with targeted pyrosequencing, E-ice-COLD-PCR has a reported average sensitivity of 0.06-0.12% mutant in a wild type background (How Kit et al., 2013).

2 AIM OF THE STUDY

The general purpose of the study was to develop and validate a new diagnostic method for assessing the mutation status of *KRAS* proto-oncogene in mCRC by using plasma as a source of DNA. The target gene and study cohort were both chosen because of direct clinical implications: only mCRC patients whose tumors have been confirmed not to contain activating RAS mutations are eligible for treatment with anti-EGFR mAbs. Furthermore, while the comprehensive analysis of *KRAS* and *NRAS* exons two, three and four is currently recommended, approximately 80% of all RAS mutations found in colorectal cancer reside in *KRAS* codons 12 and 13, giving these codons the highest priority in clinical testing and making them the primary target when developing new testing methods.

Diagnostic *KRAS* mutation testing is usually conducted using DNA from formalin fixed, paraffin embedded tissue samples. The benefits of liquid biopsy include quicker, easier and less invasive sampling that may also take into account the inter- and intratumoral clonal heterogeneity of cancer. Possible secondary uses for ctDNA-based testing include detecting residual disease after a curative surgery, tracking disease progression and predicting the emergence of acquired resistance to therapeutic agents.

The amount of ctDNA in blood is typically rather low. For this reason, the new test was developed around E-ice-COLD-PCR, a PCR-based method that selectively amplifies different low-frequency allele variants in a sample of DNA. The aim was to decrease the detection limit of allele quantification by targeted pyrosequencing from the usual 10% by one to two orders of magnitude, down to 0.1-1% of mutant DNA in a wild type background. An additional goal was the optimization of the cfDNA extraction protocol to support clinical mutation testing. We hypothesized that by using stronger relative centrifugal fields and multiple consecutive centrifugation steps for plasma separation, we could minimize the amount of hematopoietic cells and subsequent genomic DNA contamination in the samples.

Specific aims of the study:

1. To develop and optimize an E-ice-COLD-PCR assay for the selective amplification of mutations in codons 12 and 13 of human *KRAS*

2. To optimize plasma cfDNA extraction (in particular, plasma centrifugation) for clinical mutation testing

3. To validate E-ice-COLD-PCR-enhanced targeted pyrosequencing of plasma cfDNA for clinical *KRAS* mutation testing

3 MATERIALS AND METHODS

3.1 Mutant DNA and dilution series

Commercial human genomic DNA HD374 and HD376, each containing a different activating mutation in *KRAS* (c.35G>A/p.G12D and c.35G>C/p.G12A, respectively), were purchased from Horizon Diagnostics (Horizon Discovery Ltd., Cambridge, UK). Unmethylated Human Control DNA (mat. no. 1063936; Qiagen N.V., Venlo, Limburg, Netherlands) was used as wild type DNA. Upon receipt, the DNA was quantified with a Nanodrop 2000c spectrophotometer (Thermo Scientific, Wilmington, DE, USA) and corresponding allele frequencies were verified by conventional PCR followed by pyrosequencing as described in sections 3.6 and 3.8. Both mutants were diluted in wild type DNA and nuclease-free water to the following mutant allele frequencies: 0%, 0.1%, 0.25%, 0.5%, 1% and 10%. The final DNA concentration was 1 ng/µl for each sample.

3.2 Study cohort

16 patients with mCRC and undergoing chemotherapy, molecularly targeted therapy or best palliative care were recruited to the study. Each patient's tumor(s) had been screened for mutations in *KRAS* codons 12, 13 and 61 prior to the study by analyzing DNA extracted from tissue samples. When applicable, total tumor burden at the time of sampling was estimated according to RECIST 1.1 guidelines from the most recent computerized tomography or positron emission tomography scans. Each tumor was measured in three dimensions (excluding non-measurable tumors and lymph nodes, i.e. <10 mm in all three dimensions and/or diffuse), and tumor volume was approximated using the formula for an ellipsoid volume. All patients gave written informed consent and the study protocol was approved by the Central Finland Health Care District Research Ethics Committee (Reference number: Dnro 7U/2013). Characteristics of the study cohort are further detailed in Table 1 and Appendix I.

Table 1. Main characteristics of the study population. *KRAS* mutations had been assessed prior to the study by analyzing DNA from tissue samples.

mCRC patients		n = 16	
Sex	Male	7	43.8%
	Female	9	56.2%
Age	≤65	11	68.8%
	>65	5	31.2%
Location of primary tumor	Colon	11	68.8%
	Rectum	5	31.2%
KRAS mutation status	Wild type	9	56.2%
	Mutant[1]	7	43.8%

[1]Includes six mutations in codons 12 and 13 (c.34G>A, c.38G>A, c.38G>A, c.35G>T, c.35G>T and c.35G>A) and one in codon 61 (c.183A>C).

3.3 Sampling and plasma separation

Just preceding the administration of an intravenous infusion of a cycle of chemotherapeutic agents and/or molecularly targeted cancer therapeutics, peripheral blood was drawn from each patient into four 3 ml vacuum tubes containing 5.4 mg K_2EDTA (BD Vacutainer®). The venipuncture was performed by a trained biomedical laboratory scientist. Within one hour, the tubes were centrifuged for 10 min at room temperature to separate plasma from the cells. Two of the tubes were centrifuged at 500 x g, while the remaining two were centrifuged at 1,600 x g. From each sample, plasma was then carefully transferred into a clean 50 ml conical tube.

Immediately following the first centrifugation, two of the four samples (one that was centrifuged at 500 x g and one that was centrifuged at 1,600 x g) were centrifuged again at 16,000 x g for 10 min at room temperature (Fig. 5). Supernatants were transferred into clean 50 ml conical tubes while approximately 5 mm of liquid per sample was left in the original tube and discarded.

	1st centrifugation (10 min/RT)	
	500 x g	1,600 x g
2nd centrifugation (10 min/RT) -	A	B
16,000 x g	C	D
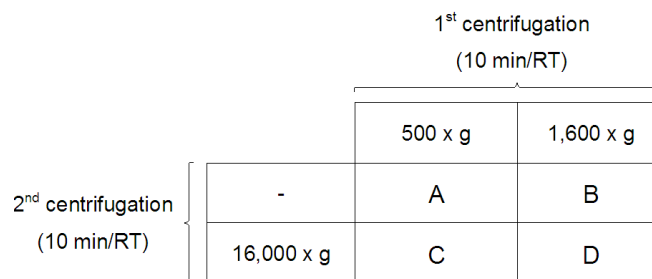
Figure 5. Plasma separation by four different centrifugation protocols. The four tubes of EDTA-blood drawn from each patient were centrifuged according to different protocols to yield plasma samples A, B, C and D.

3.4 cfDNA extraction and analysis

cfDNA extraction was carried out using a QIAamp® Circulating Nucleic Acid Kit, vacuum manifold (QIAvac® 24 plus and QIAvac® connecting system) and QIAGEN Vacuum Pump (Qiagen) according to the manufacturer's instructions. Each extraction was conducted using 1 ml of plasma, and poly-A carrier RNA was used in accordance with the manufacturer's recommendations. Samples were eluted in 50 µl of buffer AVE (essentially RNase-free water that contains sodium azide as a preservative).

Extracted cfDNA was quantified using a Qubit® 2.0 fluorometer and dsDNA High Sensitivity Assay (Life Technologies, Carlsbad, CA, USA). cfDNA yield and integrity were both assessed by capillary electrophoresis using a 2200 TapeStation Nucleic Acid System, High Sensitivity D1K ScreenTape and High Sensitivity D1K Reagents (Agilent Technologies, Santa Clara, CA, USA). The results were analyzed using TapeStation Software v. A.01.04 (Agilent Technologies).

3.5 Primer and reference strand design

Primers for amplifying (KRAS12/13_F, KRAS12/13_R) and sequencing (KRAS12/13_S) *KRAS* codons 12 and 13 were designed using PyroMark[TM] Assay Design v. 2.0.1.15 (Qiagen) (Table 2, Appendix II). The absence of detrimental secondary structures was confirmed with mFold (Zuker, 2003), and possible mispriming sites were assessed using Primer BLAST (Ye et al., 2012). The primers were purchased from TibMolBiol (Berlin, Germany). Upon receipt, the

oligos were quantified and their purity was confirmed using a Nanodrop 2000c spectrophotometer. Annealing temperatures were confirmed by a gradient PCR in a T-100 thermocycler (Bio-Rad, Hercules, CA, USA). The products were quantified using a Qubit® 2.0 fluorometer and dsDNA High Sensitivity Assay to assess reaction performance at each hybridization temperature, and the highest temperature displaying robust DNA amplification was chosen for subsequent reactions. The absence of secondary PCR products was confirmed by capillary electrophoresis using a 2200 TapeStation Nucleic Acid System, High Sensitivity D1K ScreenTape and High Sensitivity D1K Reagents. The results were analyzed using TapeStation Software v. A.01.04.

Table 2. Primers and reference strands used in the study. KRAS12/13_R features a biotin molecule to enable sequencing with a PyroMark™ Q24 pyrosequencing instrument as described in section 3.8.

Name	Application	Sequence (5' → 3')
KRAS12/13_F	Amplification of *KRAS* codons 12 and 13 (conventional and E-ice-COLD-PCR)	TATTTTTATTATAAGGCCTGCTG
KRAS12/13_R		biotin-CTCTATTGTTGGATCATATTCGT
KRAS12/13_S	Sequencing of *KRAS* codons 12 and 13 (conventional and E-ice-COLD-PCR)	ACTTGTGGTAGTTGGAGC
KRAS12/13_E-ICE_RS	Enrichment of allele variants in *KRAS* codons 12 and 13 (E-ice-COLD-PCR)	CAAGGCACTCTTGCCTAC+G+C+CA+C+C+AGCTCCAACTACCACA-phosphate

+N = LNA base

A reference oligonucleotide (KRAS12/13_E-ICE_RS) was designed for the *KRAS* E-ice-COLD-PCR assay (Table 2, Appendix II). The RS did not overlap with the PCR primers, as recommended by How Kit et al. (2013). Six LNA bases were included around codons 12 and 13, chosen so as to maximize the difference in melting temperature between a perfect match and a single-nucleotide mismatch. Each RS was linked to a 3'-phosphate group to prevent elongation by DNA polymerases. The RSs were purchased from TibMolBiol. Upon receipt, they were quantified and their purity was confirmed using a Nanodrop 2000c spectrophotometer, Qubit® 2.0 fluorometer and ssDNA Assay (Life Technologies).

3.6 Conventional PCR

PCR amplification of *KRAS* codons 12 and 13 was conducted in a T-100 thermocycler using a therascreen® KRAS Pyro® Kit (Qiagen) with the manufacturer's primers (used in the validation of HD374, HD376 and wild type genomic DNA allele frequencies) or a PyroMark^{TM} PCR Kit (Qiagen) with custom PCR and sequencing primers as described in section 3.5 (used in the assessment of primer function and optimal annealing temperatures).

Amplification with the therascreen® KRAS Pyro® Kit was performed according to the manufacturer's instructions. Briefly, 5 ng of DNA was used as a template in a 25-µl PCR mix including 1x PyroMark^{TM} PCR Master Mix (1.5 mM final $MgCl_2$ concentration), 1x CoralLoad® Concentrate and 1 µl of the manufacturer's PCR Primer KRAS 12/13. An initial activation step of 15 min at 95 °C was conducted, followed by 42 cycles of 20 sec denaturation at 95 °C, 30 sec annealing at 53 °C and 20 sec extension at 72 °C. Finally, a five-minute extension at 72 °C was performed, after which the sample was cooled and kept at 10 °C.

When conducting PCR with the PyroMark^{TM} PCR Kit, the manufacturer's primers were substituted for 0.2 µM of primers KRAS12/13_F and KRAS12/13_R. The PCR was performed as described above, except that the annealing was conducted for 30 sec at a temperature gradient of 53 °C to 58 °C.

3.7 E-ice-COLD-PCR

A T-100 thermocycler was used for the E-ice-COLD-PCR reactions. The assay was optimized as recommended by How Kit et al. (2013), i.e. an optimal T_c was determined by amplifying serial dilutions of *KRAS* c.35G>A and c.35G>C with a gradient T_c. Additional experiments using different molarities of the RS (10 nM - 30 nM) were conducted, and parameters corresponding to the strongest mutation enrichment combined with robust wild type sample amplification and limited background signal were chosen for subsequent reactions. The absence of secondary PCR products was confirmed by capillary electrophoresis using a 2200 TapeStation Nucleic Acid System, High Sensitivity D1K ScreenTape and High Sensitivity D1K Reagents. The results were analyzed using TapeStation Software v. A.01.04.

5 ng of DNA was used as a template in a 25-µl PCR mix including 1x PyroMark^{TM} PCR Master Mix, 1x CoralLoad® Concentrate, 0.2 µM of each primer (KRAS12/13_F and KRAS12/13_R) and 10 nM of KRAS12/13_E-ICE_RS. An initial activation step of 15 min at 95 °C was conducted, followed by six cycles of conventional PCR (20 sec denaturation at 95 °C, 30 sec annealing at 53 °C and 20 sec extension at 72 °C), followed by 44 cycles of E-ice-COLD-PCR (20 sec denaturation at 95 °C, 1 min RS annealing at 70 °C, 20 sec at $T_c = 80$ °C, 30 sec primer annealing at 53 °C and 20 sec extension at 72 °C). Finally, a five-minute extension at 72 °C was performed, after which the sample was cooled and kept at 10 °C.

3.8 Allele quantification by pyrosequencing

The biotin-conjugated reverse DNA strands from 10 µl of PCR product were captured on streptavidin-coated Sepharose beads (GE Healthcare, Little Chalfont, Buckinghamshire, UK), purified and rendered single stranded on a PyroMark^{TM} Q24 Vacuum Workstation (Qiagen) according to the manufacturer's instructions. DNA amplified with the therascreen® KRAS Pyro Kit was then resuspended in 25 µl of PyroMark^{TM} Annealing Buffer containing 0.8 µl of the manufacturer's sequencing primer. The sample was incubated at 80 °C for 2 min, after which it was left at room temperature for 10 min to let the primers anneal to the template. DNA amplified with the PyroMark^{TM} PCR Kit and primers KRAS12/13_F and KRAS12/13_R, including all E-ice-COLD-PCR products, was resuspended in 25 µl of PyroMark^{TM} Annealing Buffer containing 0.3 µM of primer KRAS12/13_S. The sample was then incubated at 80 °C for 2 min and left at room temperature for 20 min.

Allele quantification was performed with a PyroMark^{TM} Q24 pyrosequencing instrument and PyroMark^{TM} Gold Q24 Reagents (Qiagen). Results were analyzed with PyroMark Q24 v. 2.0.6 software (Qiagen) in allele quantification ("AQ") mode. For samples amplified with the therascreen® KRAS Pyro® Kit, a dispensation order of TACGACTCAGATCGTAG was used. The analyzed sequences were GNTGRCGTAGGC and NGTGRCGTAGGC. For all the other samples, the dispensation order was GTCAGACTCGATCGTA and the analyzed sequences were TGNTGRCGTAGGC and TNGTGRCGTAGGC. A peak height threshold was set at 30 units.

3.9 Data analysis and statistical methods

All mutations were called manually, i.e. no commercial software plug-ins were used. For mutations in *KRAS* codons 12, 13 and 61 (c.34G>T, c.34G>A, c.34G>C, c.35G>A, c.35G>T, c.35G>C, c.38G>A, c.181C>G, c.182A>T, c.182A>G, c.183A>C, c.183A>T) of the samples amplified with the therascreen® KRAS Pyro® Kit, the limit of blank (LOB) and limit of detection (LOD) were both given by the manufacturer. For samples amplified with E-ice-COLD-PCR, LOB values were determined by a non-parametric approach based on ordered values and their linear interpolation as recommended in the Clinical and Laboratory Standards Institute Guideline EP17-A, "Protocol for determination of limits of detection and limits of quantitation; approved guideline" (NCCLS, 2004). Unmethylated Human Control DNA (Qiagen) was used as the blank (n = 33) and α error was set at 5%. Analytical sensitivity was measured by comparing results from the blank samples and serial dilutions using a two-tailed Wilcoxon rank sum test. LOD values were estimated for c.35G>A and c.35G>C using the non-parametric analysis of ordered values (n = 6), while β error was set at 5%.

The cfDNA samples were tested for *KRAS* mutations in a blinded fashion. To be called mutation positive a sample had to yield a final mutant allele frequency greater or equal to LOB + 5%. Samples with mutant allele frequencies greater than LOB but less than LOB + 5% were tested again in duplicate. If both results were greater than LOB, the sample was scored mutation positive.

Statistical analysis was conducted using IBM® SPSS® Statistics 20 software (IBM Corp., Armonk, NY, US). Differences in mutant enrichment between respective dilutions of c.35G>A and c.35G>C were analyzed using a two-tailed Wilcoxon rank sum test. The degree of linear correlation between the initial mutant allele frequency and test response was estimated by a Pearson correlation coefficient. Differences between the cfDNA yields associated with the different centrifugation protocols were assessed using a Kruskal-Wallis one-way analysis of variance and a Friedman's test for correlated samples. Post-hoc analysis for the Friedman's test was conducted using a two-tailed Wilcoxon signed-rank test with a nominal P-value of 0.05 corrected for multiple comparisons using a sequential Holm-Bonferroni correction. In all other cases a P-value of 0.05 was considered statistically significant.

4 RESULTS

4.1 E-ice-COLD-PCR assay performance

KRAS mutants c.35G>A and c.35G>C were diluted to 0.1%, 0.25%, 0.5%, 1.0% and 10.0% using wild type genomic DNA. The serial dilutions were amplified with E-ice-COLD-PCR and the products underwent allele quantification by targeted pyrosequencing. Strong mutant allele enrichment was observed across the whole range of dilutions: the minimum average enrichment was approximately 5-fold for 10.0% c.35G>C and the maximum approximately 37-fold for 0.5% c.35G>A (Fig. 6a, Appendix III). c.35G>A was enriched slightly more than c.35G>C, although the difference was statistically significant only when the 0.5% and 10.0% dilutions were compared (P = 0.01 and P = 0.029, respectively). The highest mutant allele frequency, 64.3 ± 1.2%, was measured for 10.0% c.35G>A (Fig. 6b). No secondary PCR products were detected by capillary electrophoresis (data not shown).

KRAS c.35G>A and c.35G>C both displayed high linear correlation between the initial mutant frequency and the allele frequency measured after E-ice-COLD-PCR ($R^2 = 0.94$ for c.35G>A and $R^2 = 0.93$ for c.35G>C) (Fig. 6c). Samples with lower initial mutation yields generally presented with higher variance and the distribution of the dilutions was heavily skewed due to the 10.0% mutants. For this reason, the linear correlation was calculated again after excluding any results from 10.0% c.35G>A and 10.0% c.35G>C (Fig. 6d). The new coefficient of determination was 0.67 for c.35G>A and 0.55 for c.35G>C, indicating moderate linear correlation in the case of more diluted samples.

The level of background signal present in the E-ice-COLD-PCR-enhanced targeted pyrosequencing assay was quantified by analyzing a series of blank samples. LOB values were determined for the seven most common activating mutations in *KRAS* codons 12 and 13 (Table 3). When α error was set at 5%, the LOB values varied from 1.31% (c.34G>C) to 4.87% (c.38G>A). When the data from the enrichment experiments were compared to the LOB values, the assay had an analytical sensitivity of 0.1% for c.35G>A (P = 0.011) and 0.25% for c.35G>C (P < 0.001). The LOD (β = 0.05) was estimated as 0.25% for c.35G>A and 0.5% for c.35G>C.
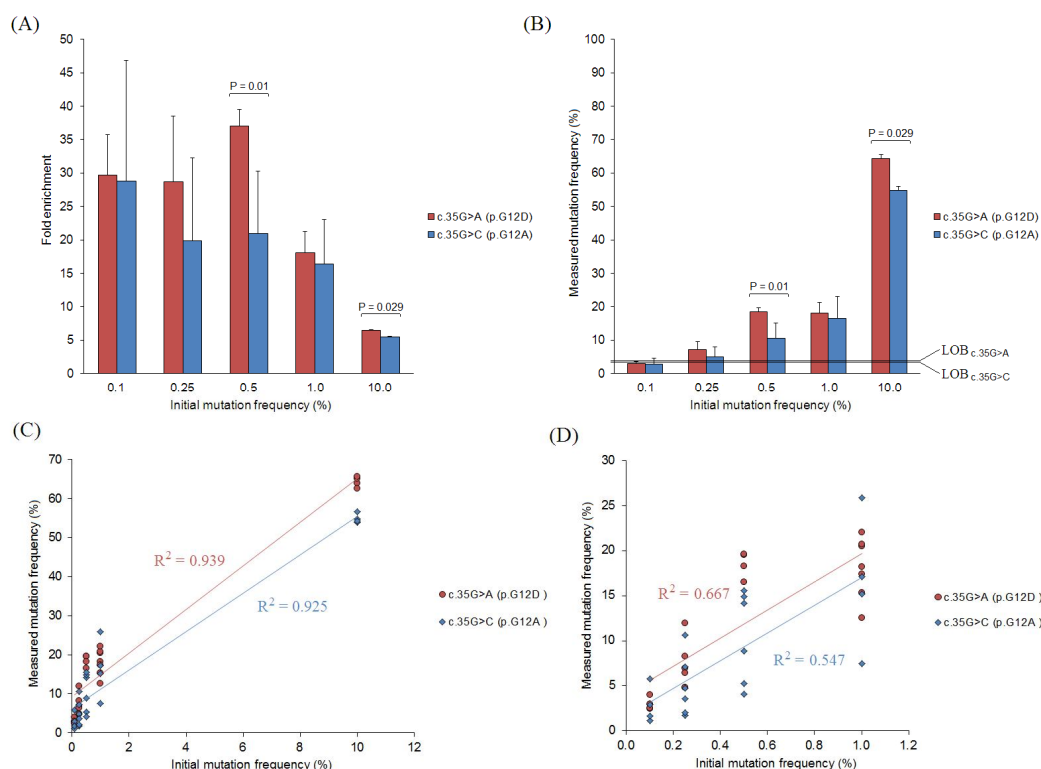
Figure 6. Technical performance of the E-ice-COLD-PCR assay. Red denotes c.35G>A (p.G12D) and blue c.35G>C (p.G12A). (A) Fold enrichment of the *KRAS* mutant alleles, relative to the initial dilution ($\bar{x} \pm$ sd; n = 4-7). (B) Measured frequency of the *KRAS* mutant alleles against a wild type background after the E-ice-COLD-PCR ($\bar{x} \pm$ sd; n = 4-7). The horizontal lines denote the LOB values of both mutants. (C) Linear correlation between the initial and measured mutation frequency for all dilutions. Each line represents the (least squares) linear trend for a given data set (i.e. mutant). (D) Linear correlation between the initial and measured mutation frequency for the 0.1%, 0.25%, 0.5% and 1.0% dilutions.

Table 3. LOB values for the E-ice-COLD-PCR assay. Depicts the maximum background signal observed for seven common base substitutions in *KRAS* codons 12 and 13 (α = 0.05).

Mutation	Limit of Blank (%)
c.34G>T (p.G12C)	1.736
c.34G>A (p.G12S)	3.880
c.34G>C (p.G12R)	1.310
c.35G>A (p.G12D)	3.982
c.35G>T (p.G12V)	3.351
c.35G>C (p.G12A)	3.598
c.38G>A (p.G13D)	4.868

4.2 cfDNA yields and integrity

The EDTA-blood drawn from each patient was centrifuged according to four discrete centrifugation protocols to separate plasma from the cells. cfDNA was extracted and the yields were measured with a fluorometer to determine the respective concentration of cfDNA in each patient's blood (Fig. 7). In the case of one patient, only a single tube of blood could be retrieved and this was processed according to protocol D. Furthermore, one C-sample was excluded from the quantitative analysis due to an error in the cfDNA elution process.
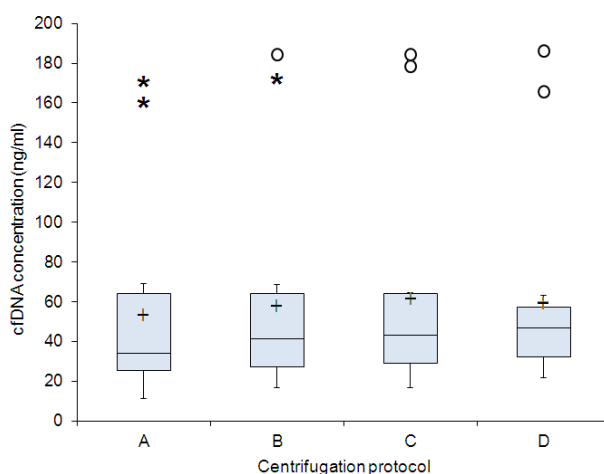
Figure 7. The amount of cfDNA in the blood samples. Values were calculated from the extracted yields. A (n = 15), B (n = 15), C (n = 14) and D (n = 16) denote the different centrifugation protocols used for plasma separation (500 x g; 500 x g + 16,000 x g; 1,600 x g; and 1,600 x g + 16,000 x g, respectively). * = outlier (upper quartile + 1.5 x IQR); o = extreme outlier (upper quartile + 3.0 x IQR); + = arithmetic mean.

The average cfDNA concentration in the blood samples was 59 ± 50 ng/ml ($\bar{x}$ ± sd). 14 patients presented with concentrations lower than 70 ng/ml, while the remaining two outliers had average cfDNA concentrations of 176 ng/ml and 175 ng/ml, respectively. No difference was observed between the cfDNA concentration distributions associated with the different centrifugation protocols (P = 0.824). However, when the samples were correlated according to individual patients, the concentrations associated with each protocol were found to be dissimilar (P = 0.022). No definitive pairwise differences were detected in the post-hoc analysis, although the comparisons between protocols A and C, A and D, and A and B approached statistical significance (P = 0.009 vs. P = 0.008, P = 0.025 vs. P = 0.01, and P =

0.049 vs. P = 0.013, respectively). The overall tumor burden varied widely between the patients, from approximately 0.6 to 225 cm^3 (Appendix I).

When the cfDNA was analyzed using capillary electrophoresis, two discrete bands were observed in every sample. These bands averaged approximately 125 bp and 700-900 bp in size. However, the electrophoresis reads were generally of low quality: signal intensities of upper (1,500 bp) and lower (25 bp) markers were low and the peaks were shifted and partially excluded from the electropherograms, preventing reliable quantitative analysis of the results (Fig. 8). A total of eight samples were analyzed before the experiment was discontinued.
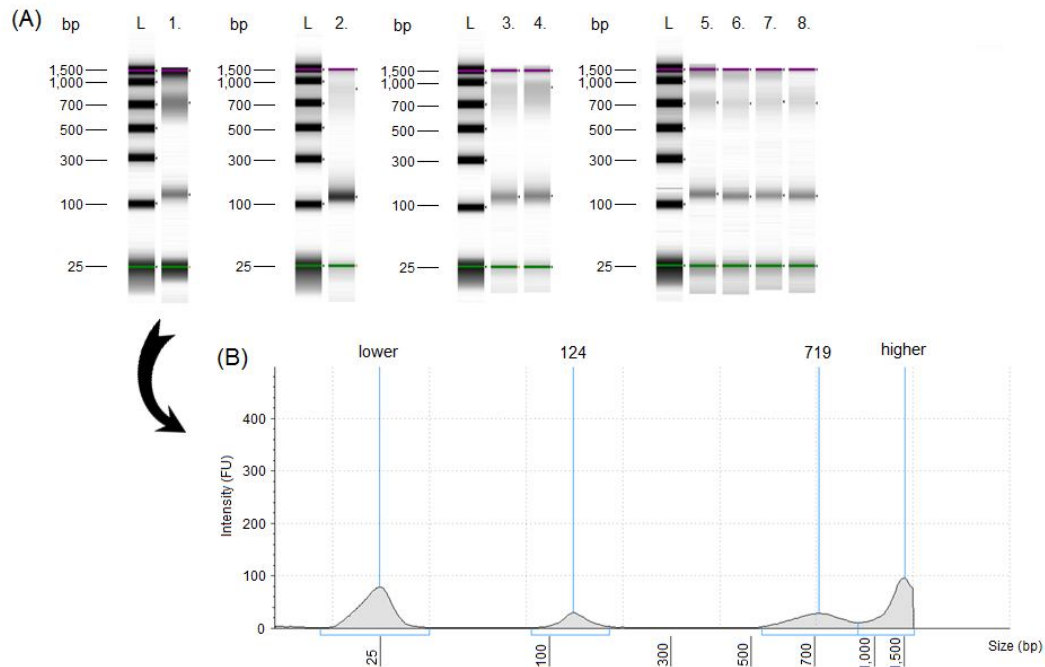
Figure 8. Capillary electrophoresis of the extracted cfDNA. (A) Eight cfDNA samples extracted from the blood of four patients. Purple and green lines denote the upper and lower DNA markers used for aligning the samples and providing quantitative information. During the analysis, some markers and/or samples were shifted relative to their respective ladder and some peaks went undetected (e.g. capillary number two). The samples from left to right: L) 3 μl of High Sensitivity D1K Ladder, 1) 1.5 ng of sample #10-D, 2) 6.6 ng of sample #12-D, 3) 6.4 ng of sample #9-A, 4) 7.5 ng of sample #9-D, 5) 2.8 ng of sample #6-A, 6) 2.5 ng of sample #6-B, 7) 2.4 ng of sample #6-C, and 8) 2.3 ng of sample #6-D. (B) Electropherogram of capillary number one (#10-D). The overall signal intensity is low and the upper DNA marker has been partially excluded from the analysis.

During the process of cfDNA extraction, poly-A carrier RNA was eluted into the cfDNA samples to an approximate final concentration of 20 ng/µl. To rule out non-specific binding to the label and/or other detrimentary effects during the capillary electrophoresis, three dilutions (200 ng/µl, 20 ng/µl and 2 ng/µl) of carrier RNA in elution buffer AVE were analyzed separately from DNA (Fig. 9). No bands were detected, while the upper and lower DNA markers were clearly defined and their signal intensity was good.
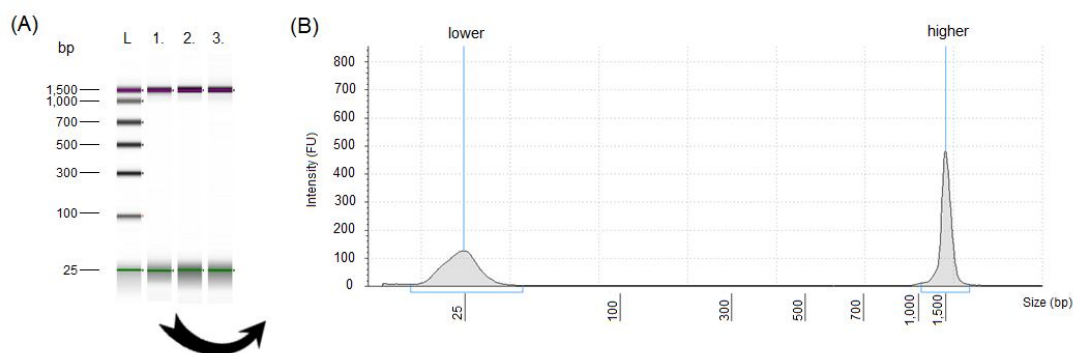
Figure 9. Capillary electrophoresis of the poly-A carrier RNA. (A) Serial dilutions of the poly-A carrier RNA used in the cfDNA extraction were analyzed using capillary electrophoresis. Purple and green lines denote the upper and lower DNA markers. The samples from left to right: L) 3 µl of High Sensitivity D1K Ladder, 1) 400 ng of carrier RNA, 2) 40 ng of carrier RNA, 3) 4 ng of carrier RNA. (B) Electropherogram of capillary number one (400 ng of carrier RNA). Besides the DNA markers, no peaks were detected.

4.3 Diagnostic parameters

Each sample from the sample set A (n = 15) was tested for *KRAS* codon 12 and 13 mutations using the E-ice-COLD-PCR-enhanced targeted pyrosequencing assay. Two of the samples, #4-A and #6-A, were deemed mutation positive (for c.35G>C (p.G12A) and c.38G>A (p.G13D), respectively). The observed mutant allele frequencies following E-ice-COLD-PCR were 11.8 % for #4-A and 6.7 % for #6-A. When the results were compared to the true mutation statuses of each respective patient, the assay had a sensitivity of 17%, a specificity of 89% and an overall accuracy of 60% (Fig. 10).

	Assay$^+$	Assay$^-$	Total
KRAS$^+$	1	5	6
KRAS$^-$	1	8	9
Total	2	13	15

Sensitivity	17 %
Specificity	89 %
Positive predictive value (precision)	50 %
Negative predictive value	62 %
Accuracy	60 %

Figure 10. Diagnostic parameters of *KRAS* mutation testing by E-ice-COLD-PCR-enhanced targeted pyrosequencing of plasma cfDNA. True *KRAS* mutation statuses (*KRAS*$^+$/*KRAS*$^-$) had been assessed prior to the study by analyzing DNA from tissue specimen. Assay refers to the current assay.

In order to evaluate whether the plasma centrifugation protocol had an effect on the test performance, samples B, C and D corresponding to the two mutation positive A-samples were assayed in duplicate. Sample #6-B tested positive for c.38G>A in both occasions and sample #6-C once, while no mutations were detected in samples #6-D, #4-B, #4-C and #4-D. Furthermore, none of the other remaining D-samples tested positive for *KRAS* codon 12 or 13 mutations.

5 DISCUSSION

Conventional cancer treatments have been complemented by an increasing number of novel molecularly targeted therapeutics. By targeting cancer-specific alterations in cellular metabolism and inter- and intracellular signaling, researchers and physicians hope to achieve better treatment efficacies and more favorable drug toxicity profiles. The results have been encouraging, although some considerable challenges associated with the new therapeutics still remain (Huang et al., 2014). One of them is the need for reliable predictive biomarkers. Intracellular signaling pathways are intrinsically complex and the response rate to a targeted therapy across an unselected patient population is usually relatively small. Mutations in the ERK cascade are a prime example: when EGFR-expressing colorectal cancer is treated with anti-EGFR mAbs, *KRAS* mutation status is a strong predictive biomarker for treatment response, progression-free survival and overall survival (Bokemeyer et al., 2011; Douillard et al., 2013).

Here we report the development and optimization of an in-house E-ice-COLD-PCR-enhanced targeted pyrosequencing assay for the sensitive detection of oncogenic mutations in *KRAS* codons 12 and 13. The goal of the study was to enable the rapid and non-invasive diagnostic mutation testing of mCRC patients using plasma cfDNA as starting material. 16 mCRC patients were recruited to validate the test performance in a clinical setting. The role of plasma separation in cfDNA extraction and subsequent mutation testing was also studied. A lack of standardized methods holds back the research on cfDNA (Jung et al., 2010), and our aim was to ascertain whether the choice of a centrifugation protocol can affect the final cfDNA yield and integrity, or the suitability of the sample for diagnostic mutation testing in general.

The assay proved highly selective and efficient, displaying robust enrichment of *KRAS* allele variants c.35G>A and c.35G>C. The maximum analytical sensitivity was 0.1-0.25% mutant in a wild type background, while the LOD was estimated as 0.25-0.5%. A moderate linear correlation was observed between the initial allele frequency and respective test response, leading to semi-quantitative results. The average amount of cfDNA detected in each patient's blood was 59 ng/ml, which was concordant with previous studies on advanced colorectal cancer. The association between centrifugation and subsequent cfDNA yields and/or integrity

was negligible, although the samples that were centrifuged once at 500 x g generally contained slightly less DNA than any of the correlated samples. The same samples also seemed to result in more sensitive *KRAS* mutation testing. However, due to the small sample size these results were exploratory at best. The overall accuracy of the assay was 60%, with a sensitivity of 17% and a specificity of 89%.

5.1 Sensitive and semi-quantitative detection of KRAS exon two mutations

Ideally, the optimization of E-ice-COLD-PCR should be conducted separately for all the mutations of interest. In the current study this was not feasible due to time and budget constraints. *KRAS* mutants c.35G>A and c.35G>C were used in the assay development and optimization for two reasons. First, c.35G>A is the most prevalent *KRAS* mutation in colorectal cancer (Fig. 2). Physicians are more likely to benefit from the assessment of exact LOD values and response linearity if these parameters are linked to commonly observed alterations. Second, both mutations have different effects on the amplicon melting temperature. Five out of the seven most common *KRAS* codon 12 and 13 mutations (c.34G>T, c.34G>A, c.35G>A, c.35G>T, c.38G>A) lower the DNA strand's melting temperature, as a guanine is replaced by an adenine or thymine. The remaining two mutations (c.34G>C, c.35G>C) do not have similar direct effects on the melting temperature. Even though E-ice-COLD-PCR is considered very robust against mutation-specific thermodynamic effects (How Kit et al., 2013), we confirmed this by choosing mutations with both G/C→A/T and G/C→G/C base changes.

All the *KRAS* c.35G>A and c.35G>C dilutions displayed efficient mutation enrichment when amplified and analyzed using E-ice-COLD-PCR-enhanced targeted pyrosequencing (Fig. 6a,b). In concordance with How Kit et al. (2013), stronger relative enrichment was observed in samples with a lower initial mutant allele frequency. Even so, 0.1% dilutions rarely presented with final mutant frequencies above their respective LOB, making the accurate measurement of their allele enrichment difficult and necessitating a careful interpretation of the results presented in Figure 6a. The LOB values themselves were relatively high (Table 3), more so than the background signal observed in conventional PCR reactions conducted using primers KRAS12/13_F and KRAS12/13_R (data not shown). However, the three base changes with

the highest LOB values (c.38G>A, c.35G>A and c.34G>A) were all variants in which adenine replaces another nucleotide in the sequence. A part of the observed background may possibly be attributed to the enzyme luciferase using minute amounts of dATPαS directly for the light producing synthesis of oxyluciferin (Zhou et al., 2005). Indeed, significant background signal in adenine positions has been reported by How Kit et al. (2013).

Alleles containing mutation c.35G>A were enriched slightly more than those harboring c.35G>C (Fig. 6a,b). The difference was relatively small but statistically significant. This is discordant with the mutant allele enrichment reported by How Kit et al. (2013): their *KRAS* assay amplified both mutants with similar efficiency, although the maximum analytical sensitivity was 0.1% for c.35G>C and 0.01% for c.35G>A. However, this was mainly due to a slight difference in the background signal between the two base alterations. It is also interesting to note that our results seem to contradict the basic thermodynamic properties of specific LNA-DNA mismatches. +C•C mismatches, such as the one present in the RS-c.35G>C heteroduplex (+C+CA/GCT), tend to lower the dimer's melting temperature more than +C•A mismatches in otherwise similar sequences (e.g. RS-c.35G>A; +C+CA/GAT) (Owczarzy et al., 2011; You et al., 2006). This effect is essentially greater than any thermodynamic change induced by the base mutation type (G/C→A/T or G/C→G/C), as discussed above. Whether the difference should be expected to have any impact on the actual E-ice-COLD-PCR performance is open to speculation.

The maximum analytical sensitivity of our E-ice-COLD-PCR-based *KRAS* mutation test was 0.1% for c.35G>A and 0.25% for c.35G>C. While this is impressive in its own right, the values were slightly higher than those displayed by the original E-ice-COLD-PCR-enhanced *KRAS* mutation detection assay (How Kit et al., 2013). The difference can be attributed to the combined effect of more efficient mutation enrichment and a slightly lower overall background signal. In a clinical setting the analytical sensitivity is secondary to LOD, which defines the lowest concentration of analyte that is consistently (i.e. in terms of acceptable β error) detected by the test. We estimated the LOD as 0.25% for c.35G>A and 0.5% for c.35G>C. Indeed, none of the individual samples at or above these LOD thresholds were scored negative by our test. However, the sample sizes were modest and care should be taken when interpreting these results.

The mutant allele frequency measured by our assay has at least three potential sources of stochastic variation: the number of mutant strands that originally end up in the assay, actual E-ice-COLD-PCR performance and the final pyrosequencing step. The variation in the initial mutant allele frequency is a more decisive factor in highly diluted samples. In fact, five nanograms of DNA typically comprise approximately 1500 genomic equivalents. The probability that no mutants actually end up in the reaction mixture during the test can be inferred from a Poisson distribution; when the mutant allele fraction of the sample is 0.1%, the probability of a "null" test sample being selected is close to 20%. This scarcity of mutant alleles establishes a definitive lower limit for the LOD of any diagnostic mutation test that analyzes small amounts of DNA.

We estimated the degree of linear correlation between the initial mutation frequency and respective assay response (i.e. the mutation frequency measured after E-ice-COLD-PCR) to find out whether the test can be used for estimating the true mutant allele frequency in a sample of DNA. The results indicated a high degree of linearity or, after excluding the data from 10.0% c.35G>A and 10.0% c.35G>C, a moderate degree of linear correlation for both mutants (Fig. 6c,d). Analyzing several identical samples in parallel and using the average of the results as a "true" measured frequency may further increase the accuracy of quantitative testing. This may allow test operators to detect at least the more significant changes in the patients' relative ctDNA concentrations, so long as they occur between the respective LOD and 10.0%. If the frequency is above 10.0%, conventional targeted pyrosequencing may be used instead. Nevertheless, further studies are needed to confirm the suitability of E-ice-COLD-PCR-enhanced targeted pyrosequencing for quantitative analysis, especially since no responses were measured for samples with a known mutant allele frequency between 1.0 to 10.0%.

5.2 Low-speed plasma centrifugation is not associated with increased genomic DNA contamination

The average cfDNA concentration in circulation was approximately 60 ng/ml (or 40 ng/ml after the two outliers were excluded) (Fig. 7), which is concordant with values previously reported in the context of advanced colorectal cancer (Diehl et al., 2005; Diehl et al., 2008).

There were two outliers, patients #9 and #12, with approximate cfDNA concentrations of 175 ng/ml. Both patients presented with a progressive disease combined with multiple metastases and a moderate to heavy overall tumor burden. Moreover, the measured values were still well within the confines of those previously reported for similar conditions (Diehl et al., 2005).

Contrary to the rationale behind many current cfDNA extraction protocols, adding an additional high-speed centrifugation step did not markedly lower the DNA yields by decreasing the amount of genomic DNA contamination originating from hematopoietic cells (Fig. 7). Instead, when correlated samples were compared to each other, protocol A often yielded slightly less DNA than the other centrifugation protocols. This contradicts the previously reported observation that a single centrifugation step at 1,600 x g or less does not remove all the cells and/or cellular debris from a blood sample (Chiu et al., 2001). However, our samples were smaller than the ones used in the original study (3 ml instead of 6-8 ml), which might explain at least some of the differences in sedimentation efficiency. On the other hand, effective sedimentation alone does not explain the tendency of the A-samples to yield less DNA than any of the correlated samples. A seemingly likely factor contributing to the higher DNA concentration in the more vigorously centrifuged samples is cell breakdown induced my mechanical strain. However, Lui et al. (2002a,b) have suggested that even multiple centrifugation steps at 3000 x g and 16,000 x g are insufficient to cause significant cell destruction and release of genomic DNA into the plasma.

The size distribution of circulating cfDNA fragments in both healthy individuals and cancer patients has been a target of close scrutiny. So far, the observations have often been contradictory and malignant conditions have been reported to result in both increased (Wang et al., 2003) and decreased (Ellinger et al., 2009) overall cfDNA integrity. In patients with colorectal disease (colorectal cancer or adenomatous polyps), oncogenic *KRAS* (Wang et al., 2004) and *APC* (Diehl et al., 2005) mutations are more abundant in the low molecular weight fraction of cfDNA. Indeed, Mouliere et al. (2011) have recently shown that up to 98% of the ctDNA in mCRC is made up by <400 bp fragments. The size distribution of non-tumor derived cfDNA is more even, and <400 bp fragments constitute approximately 65% of these nucleic acids.

To maximize the sensitivity of *KRAS* mutation testing, capillary electrophoresis was used to compare the fragment size distributions of the cfDNA samples extracted using different centrifugation protocols. However, the method itself performed poorly: DNA markers were distorted and misplaced and the overall fluorescence intensity was low, making the assessment of DNA concentrations impossible and casting doubt on the accuracy of the reported fragment sizes. As serial dilutions of poly-A carrier RNA in elution buffer did nothing to hamper the normal function of the electrophoresis (Fig. 9), the presence of other unspecified contaminants in the cfDNA samples seems like a viable explanation. Such contaminants would likely originate from the plasma, which warrants further validation of the silica membrane-based cfDNA extraction process.

Each of the eight cfDNA samples analyzed by the capillary electrophoresis displayed two DNA bands, averaging approximately 125 bp and between 700 and 900 bp in size (Fig. 8). Electrophoresized cfDNA often forms a characteristic ladder pattern, which mostly comprises mono-, di- and trinucleosomal cfDNA originating from apoptotic cells (Jahr et al., 2001; Wang et al., 2004). However, these fragments are typically multiples of 180 bp in size. We observed only two bands, both smaller and larger fragments than expected, and relatively little cfDNA present in other fragment sizes. The bands appeared uniform regardless of the centrifugation protocol. This suggests that the fragments originated from the actual cfDNA fraction in blood, rather than being contaminants released due to the centrifugation. Even so, the results of the electrophoresis were distorted due to the technical difficulties discussed above, and all the observations concerning DNA integrity and fragment size profiles should be interpreted with due caution.

All in all, the choice of a centrifugation protocol for separating plasma from small volumes (3 ml) of blood is not associated with any diagnostically significant differences in genomic DNA contamination. However, as a single centrifugation step at 500 x g often yielded slightly less cfDNA than the more vigorous protocols, the resulting sample set was chosen for *KRAS* mutation testing. Further studies are needed to confirm whether the observed trend in cfDNA concentrations is reproducible.

5.3 Detecting oncogenic KRAS mutations in plasma cfDNA

The study cohort comprised 16 patients, seven of whom presented with previously detected *KRAS* mutations (Table 1). However, one of the mutations resided in codon 61. Moreover, one *KRAS* mutation negative patient was excluded from the mutation analysis after the person's cfDNA could not be extracted according to protocol A. A total of 15 cfDNA samples from the sample set A were tested for *KRAS* exon two hotspot mutations using E-ice-COLD-PCR-enhanced targeted pyrosequencing.

Two pathogenic mutations, *KRAS* c.35G>C (p.G12A) and c.38G>A (p.G13D), were detected by the current assay. The test had a mediocre overall accuracy of 60% for predicting *KRAS* exon two mutation status (Fig. 10). While the specificity of the test was 89%, the sensitivity was only 17%; this is, of course, grossly inadequate for a standalone diagnostic test. As the number of mutations in the study cohort was concordant with the known prevalence across all mCRC patients (6/15→40%), positive (50%) and negative (62%) predictive values were inferred directly from the test results.

There are several possible explanations for the observed lack of accuracy. First, any given set of PCR primers used for amplifying *KRAS* codons 12 and 13 for mutation testing must not anneal to the gene too close to each other; otherwise they may also amplify pseudogene *KRASP1* (McGrath et al., 1983), which will then interfere with all the downstream analyses. The amplicon used in our assay was 137 bp in length (Appendix II). However, ctDNA from mCRC tends to be more fragmented than corresponding non-tumor derived cfDNA, and up to 70% may present in ≤100 bp fragments (Mouliere et al., 2011). Since the assay was optimized and its LOD was assessed using high integrity genomic DNA, it is possible that the practical sensitivity of the test is actually somewhat lower for cfDNA samples.

More importantly, clinical factors are likely to explain at least some of the non-concordant results. In several instances, the gold standard test used for determining the patient's *KRAS* mutation status had been conducted using DNA from a tissue sample that was taken two, three or even four years prior to the current study (Appendix I). Some of the tissue specimen were from radical surgery, in which case at least the tested sub-population of malignant cells had

been effectively eliminated from the patient's system. Furthermore, cases where a temporary withdrawal from targeted anti-EGFR therapy has resulted in the loss of acquired resistance have been reported (Sequist et al., 2011). Although these mutations were not located in *KRAS*, but rather in the kinase domain of *EGFR* itself, the observation still demonstrates that the accumulation of specific somatic mutations in individual tumors is not, by definition, an irreversible process.

The assay also detected a novel c.35G>C mutation. This variant had not been present in the tumor sample that was analyzed approximately four years prior to the study, and consequently the current mutation was reported as a false positive (Fig. 10). However, the patient had recently been receiving a combination therapy comprising panitumumab, irinotecan, fluorouracil and folinic acid. The treatment was altered after the disease once again progressed, indicating the development of acquired resistance to anti-EGFR mAbs approximately four months before the blood samples were collected. Therefore, this case may also be interpreted as an example of how cfDNA-based testing may be used to predict the emergence of acquired resistance. It also underlines the problems associated with using retrospective reference samples that have been collected at different time points. All in all, a prospective study is necessary for the comprehensive and reliable validation of cfDNA-based *KRAS* mutation testing.

The centrifugation protocol had little effect on the final cfDNA yield (i.e. the concentrations were always of the same order of magnitude), suggesting that the same might be true for *KRAS* mutation testing. However, when the B-, C- and D-samples corresponding to the two mutation positive A-samples were assayed, only some of them were scored positive. More specifically, oncogenic allele variants were found in some of the B- and C-samples, while both D-samples were determined mutation negative on two separate occasions. The more vigorous the centrifugation preceding cfDNA extraction, the lower the likelihood of mutations being detected (A>B≈C>D). This observation raises significant concerns for the practical implementation of plasma samples as a source of material for diagnostic mutation testing, warranting additional studies.

Due to the extremely small sample size, definitive conclusions on the correlation between plasma separation and the efficiency of cfDNA-based *KRAS* mutation testing could not be drawn. However, it is still worthwhile to consider one factor that may contribute to the observed difference. Many cancer cells utilize extracellular vesicles as a means of intercellular signaling: for example, microvesicles shed by glioblastoma cells may promote angiogenesis in normal brain endothelial cells and stimulate proliferation in nearby cancer cells (Skog et al., 2008). Similar angiogenic microvesicles have been reported in the context of colorectal cancer (Hong et al., 2009). In addition to proteins and RNA, vesicles shed from several cancer types have been shown to contain DNA that reflects the genetic status of the tumor, such as amplifications in oncogene *c-Myc* (Balaj et al., 2011). Furthermore, a recent study has demonstrated that *KRAS* mutation status affects the content of the colon cancer-derived microvesicles: oncogenic proteins, including mutant K-Ras itself, are enriched in vesicles originating from *KRAS* mutation positive cells (Demory Beckler et al., 2013).

If oncogenic *KRAS* sequences are also enriched in tumor-derived microvesicles, vigorous centrifugation may remove some of them and decrease the number of allele variants that end up in the final sample. At the same time, the reduction in total cfDNA yield might be negligible. Centrifugation at 500 x g would be unlikely to sediment the vesicles at all; after all, similar centrifugal fields are often used for the initial removal of cell debris during microvesicle purification (Hong et al., 2009; Yu et al., 2005). On the other hand, even centrifugation at 1,600 x g would probably be insufficient to alter the vesicle concentration. However, tumor-derived microvesicles can be taken up by platelets (Nilsson et al., 2011). Since RNA is readily transferred between the two, it is conceivable that the platelets might also contain oncogenic DNA. Moreover, platelets sediment easily, even in the presence of relatively weak centrifugal fields. Although hypothetical at this point, we propose that future studies focusing on liquid biopsy-based *KRAS* mutation testing should pay attention to the possible association between microvesicles, platelets and assay sensitivity.

5.4 Conclusions and future prospects

E-ice-COLD-PCR-enhanced targeted pyrosequencing enables robust and semi-quantitative detection of *KRAS* allele variants c.35G>A and c.35G>C. The method is cost-efficient and straightforward, as the only specialized equipment or reagents needed are the amplicon-specific primers and RSs. Moreover, the combination of low LOD and the ability to detect mutations from as little as 5 ng of DNA makes the assay a promising candidate for blood-based clinical mutation testing. While the performance of the test was not directly validated for other hotspot mutations known to occur in *KRAS* codons 12 and 13 (i.e. c.34G>T, c.34G>A, c.34G>C, c.35G>T and c.38G>A), this can be easily accomplished once a need for respective LOD values or quantitative analysis presents itself. In the meantime, the established LOB values allow for calling any of the seven mutations as they are encountered.

The low diagnostic sensitivity observed in this study contradicts previous reports of relatively high levels of tumor-derived ctDNA in advanced colorectal cancer (Diehl et al., 2005). This may be partially explained by the heterogeneity of the current study cohort, including their clinical statuses and treatment histories. Even if comprehensive prospective studies confirm this lack of sensitivity in the future, the assay may still prove useful as a secondary option for situations where a conventional biopsy is unavailable and having a test with low sensitivity is better than having no test at all.

Apart from mCRC, *KRAS* mutation status is also relevant in the context of several other human malignancies. For example, mutated *KRAS* may be a negative prognostic marker for pancreatic adenocarcinoma, non-small cell lung cancer and thyroid carcinoma, although some of these associations are still relatively controversial (Fernández-Medarde and Santos, 2011). Furthermore, small molecule EGFR inhibitors are used routinely for treating *EGFR* mutation positive non-small cell lung cancer and the inverse correlation between activating *KRAS* mutations and treatment response has only recently been appreciated (Reviewed by Karachaliou et al., 2013). Acquiring tissue biopsies from lung tumors is often difficult; if *KRAS* mutation status proves to be a viable predictive biomarker for non-small cell lung cancer, liquid biopsy may become a useful complement to the more conventional testing methods.

Mutations in *KRAS* codons 12 and 13 comprise approximately 80% of all RAS mutations in colorectal cancer. Consequently, these variants are the primary targets for mCRC-related diagnostic testing and many recent studies on sensitive RAS mutation detection have focused exclusively on *KRAS* exon two (Chang et al., 2014; Dijkstra et al., 2013; How Kit et al., 2013; Taly et al., 2013). By contrast, relatively few methods for detecting other low-frequency *KRAS* or *NRAS* mutations have been reported. Nevertheless, completely disregarding 20% of pathogenic RAS mutations is unacceptable in a clinical setting. In order to fully utilize E-ice-COLD-PCR-enhanced targeted pyrosequencing as a diagnostic tool against cancer, the assay must eventually be expanded so as to detect any of the known oncogenic mutations in *KRAS* and *NRAS* exons two, three and four.

All in all, ctDNA is proving to be an efficient and versatile biomarker for many different cancer types. One indication of this is the increasing amount of ongoing clinical trials that focus on liquid biopsy: examples include a study on ctDNA levels in relation to the dynamics and recurrence of early-stage breast cancer (NCT01617915) and another study on ctDNA-based molecular profiling of non-small cell lung cancer (NCT02169349). The new biomarkers have multiple uses, ranging from primary diagnostics and early detection to disease monitoring, predicting treatment response and more. Liquid biopsy will help advance the personalized treatment of cancer, decreasing both treatment costs and human suffering.

REFERENCES

Ascierto, P.A., J.M. Kirkwood, J.J. Grob, E. Simeone, A.M. Grimaldi, M. Maio, G. Palmieri, A. Testori, F.M. Marincola, and N. Mozzillo. 2012. The role of BRAF V600 mutation in melanoma. J.Transl.Med. 10:85-5876-10-85.

Balaj, L., R. Lessard, L. Dai, Y.J. Cho, S.L. Pomeroy, X.O. Breakefield, and J. Skog. 2011. Tumour microvesicles contain retrotransposon elements and amplified oncogene sequences. Nat.Commun. 2:180.

Basu, T., P.H. Warne, and J. Downward. 1994. Role of Shc in the activation of Ras in response to epidermal growth factor and nerve growth factor. Oncogene. 9:3483-3491.

Batista, T.P., C.A. Santos, and G.F. Almeida. 2013. Perioperative chemotherapy in locally advanced gastric cancer. Arq.Gastroenterol. 50:236-242.

Bendich, A., T. Wilczok, and E. Borenfreund. 1965. Circulating Dna as a Possible Factor in Oncogenesis. Science. 148:374-376.

Bettegowda, C., M. Sausen, R.J. Leary, I. Kinde, Y. Wang, N. Agrawal, B.R. Bartlett, H. Wang, B. Luber, R.M. Alani, E.S. Antonarakis, N.S. Azad, A. Bardelli, H. Brem, J.L. Cameron, C.C. Lee, L.A. Fecher, G.L. Gallia, P. Gibbs, D. Le, R.L. Giuntoli, M. Goggins, M.D. Hogarty, M. Holdhoff, S.M. Hong, Y. Jiao, H.H. Juhl, J.J. Kim, G. Siravegna, D.A. Laheru, C. Lauricella, M. Lim, E.J. Lipson, S.K. Marie, G.J. Netto, K.S. Oliner, A. Olivi, L. Olsson, G.J. Riggins, A. Sartore-Bianchi, K. Schmidt, l. Shih, S.M. Oba-Shinjo, S. Siena, D. Theodorescu, J. Tie, T.T. Harkins, S. Veronese, T.L. Wang, J.D. Weingart, C.L. Wolfgang, L.D. Wood, D. Xing, R.H. Hruban, J. Wu, P.J. Allen, C.M. Schmidt, M.A. Choti, V.E. Velculescu, K.W. Kinzler, B. Vogelstein, N. Papadopoulos, and L.A. Diaz Jr. 2014. Detection of circulating tumor DNA in early- and late-stage human malignancies. Sci.Transl.Med. 6:224ra24.

Bokemeyer, C., I. Bondarenko, J.T. Hartmann, F. de Braud, G. Schuch, A. Zubel, I. Celik, M. Schlichting, and P. Koralewski. 2011. Efficacy according to biomarker status of cetuximab plus FOLFOX-4 as first-line treatment for metastatic colorectal cancer: the OPUS study. Ann.Oncol. 22:1535-1546.

Chan, K.C., P. Jiang, Y.W. Zheng, G.J. Liao, H. Sun, J. Wong, S.S. Siu, W.C. Chan, S.L. Chan, A.T. Chan, P.B. Lai, R.W. Chiu, and Y.M. Lo. 2013. Cancer genome scanning in plasma: detection of tumor-associated copy number aberrations, single-nucleotide variants, and tumoral heterogeneity by massively parallel sequencing. Clin.Chem. 59:211-224.

Chang, Y.S., T.K. Er, H.C. Lu, K.T. Yeh, and J.G. Chang. 2014. Detection of KRAS codon 12 and 13 mutations by mutant-enriched PCR assay. Clin.Chim.Acta. 436C:169-175.

Chermiti Ben Abdallah, F., G. Ben Ali, M. Sadok Boudaya, M. Mlika, A. Chtourou, S. Taktak, and A. Ben Kheder. 2014. Treatment and prognosis of advanced stage non-small-cell lung cancer. Rev.Mal.Respir. 31:214-220.

Chiu, R.W., L.L. Poon, T.K. Lau, T.N. Leung, E.M. Wong, and Y.M. Lo. 2001. Effects of blood-processing protocols on fetal and total DNA quantification in maternal plasma. Clin.Chem. 47:1607-1613.

Cunningham, D., Y. Humblet, S. Siena, D. Khayat, H. Bleiberg, A. Santoro, D. Bets, M. Mueser, A. Harstrick, C. Verslype, I. Chau, and E. Van Cutsem. 2004. Cetuximab monotherapy and cetuximab plus irinotecan in irinotecan-refractory metastatic colorectal cancer. N.Engl.J.Med. 351:337-345.

Damin, D.C., and A.R. Lazzaron. 2014. Evolving treatment strategies for colorectal cancer: a critical review of current therapeutic options. World J.Gastroenterol. 20:877-887.

Dawson, S.J., D.W. Tsui, M. Murtaza, H. Biggs, O.M. Rueda, S.F. Chin, M.J. Dunning, D. Gale, T. Forshew, B. Mahler-Araujo, S. Rajan, S. Humphray, J. Becq, D. Halsall, M. Wallis, D. Bentley, C. Caldas, and N. Rosenfeld. 2013. Analysis of circulating tumor DNA to monitor metastatic breast cancer. N.Engl.J.Med. 368:1199-1209.

De Roock, W., D.J. Jonker, F. Di Nicolantonio, A. Sartore-Bianchi, D. Tu, S. Siena, S. Lamba, S. Arena, M. Frattini, H. Piessevaux, E. Van Cutsem, C.J. O'Callaghan, S. Khambata-Ford, J.R. Zalcberg, J. Simes, C.S. Karapetis, A. Bardelli, and S. Tejpar. 2010. Association of KRAS p.G13D mutation with outcome in patients with chemotherapy-refractory metastatic colorectal cancer treated with cetuximab. Jama. 304:1812-1820.

Demory Beckler, M., J.N. Higginbotham, J.L. Franklin, A.J. Ham, P.J. Halvey, I.E. Imasuen, C. Whitwell, M. Li, D.C. Liebler, and R.J. Coffey. 2013. Proteomic analysis of exosomes from mutant KRAS colon cancer cells identifies intercellular transfer of mutant KRAS. Mol.Cell.Proteomics. 12:343-355.

Diaz, L.A.,Jr, and A. Bardelli. 2014. Liquid biopsies: genotyping circulating tumor DNA. J.Clin.Oncol. 32:579-586.

Diehl, F., M. Li, D. Dressman, Y. He, D. Shen, S. Szabo, L.A. Diaz Jr, S.N. Goodman, K.A. David, H. Juhl, K.W. Kinzler, and B. Vogelstein. 2005. Detection and quantification of mutations in the plasma of patients with colorectal tumors. Proc.Natl.Acad.Sci.U.S.A. 102:16368-16373.

Diehl, F., K. Schmidt, M.A. Choti, K. Romans, S. Goodman, M. Li, K. Thornton, N. Agrawal, L. Sokoll, S.A. Szabo, K.W. Kinzler, B. Vogelstein, and L.A. Diaz Jr. 2008. Circulating mutant DNA to assess tumor dynamics. Nat.Med. 14:985-990.

Dijkstra, J.R., D.A. Heideman, G.A. Meijer, J.E. Boers, N.A. 't Hart, J. Diebold, A. Hirschmann, G. Hoefler, G. Winter, G. Miltenberger-Miltenyi, S.V. Pereira, S.D. Richman, P. Quirke, E.L. Rouleau, J.M. Guinebretiere, S. Tejpar, B. Biesmans, and J.H. van Krieken. 2013. KRAS mutation analysis on low percentage of colon cancer cells: the importance of quality assurance. Virchows Arch. 462:39-46.

Douillard, J.Y., K.S. Oliner, S. Siena, J. Tabernero, R. Burkes, M. Barugel, Y. Humblet, G. Bodoky, D. Cunningham, J. Jassem, F. Rivera, I. Kocakova, P. Ruff, M. Blasinska-Morawiec, M. Smakal, J.L. Canon, M. Rother, R. Williams, A. Rong, J. Wiezorek, R. Sidhu, and S.D. Patterson. 2013. Panitumumab-FOLFOX4 treatment and RAS mutations in colorectal cancer. N.Engl.J.Med. 369:1023-1034.

Douillard, J.Y., S. Siena, J. Cassidy, J. Tabernero, R. Burkes, M. Barugel, Y. Humblet, G. Bodoky, D. Cunningham, J. Jassem, F. Rivera, I. Kocakova, P. Ruff, M. Blasinska-Morawiec, M. Smakal, J.L. Canon, M. Rother, K.S. Oliner, M. Wolf, and J. Gansert. 2010. Randomized, phase III trial of panitumumab with infusional fluorouracil, leucovorin, and oxaliplatin (FOLFOX4) versus FOLFOX4 alone as first-line treatment in patients with previously untreated metastatic colorectal cancer: the PRIME study. J.Clin.Oncol. 28:4697-4705.

Ellinger, J., V. Wittkamp, P. Albers, F.G. Perabo, S.C. Mueller, A. von Ruecker, and P.J. Bastian. 2009. Cell-free circulating DNA: diagnostic value in patients with testicular germ cell cancer. J.Urol. 181:363-371.

Erbitux® SmPC. Summary of Product Characteristics at http://www.medicines.org.uk/emc/medicine/19595. Updated on 04.07.2014. Retrieved on 05.01.2015.

Ferlay, J., E. Steliarova-Foucher, J. Lortet-Tieulent, S. Rosso, J.W. Coebergh, H. Comber, D. Forman, and F. Bray. 2013. Cancer incidence and mortality patterns in Europe: estimates for 40 countries in 2012. Eur.J.Cancer. 49:1374-1403.

Fernández-Medarde, A., and E. Santos. 2011. Ras in cancer and developmental diseases. Genes Cancer. 2:344-358.

Finnish Cancer Registry, Cancer Statistics at http://www.cancerregistry.fi. Updated on 08.10.2014. Retrieved on 05.01.2015.

Gerlinger, M., A.J. Rowan, S. Horswell, J. Larkin, D. Endesfelder, E. Gronroos, P. Martinez, N. Matthews, A. Stewart, P. Tarpey, I. Varela, B. Phillimore, S. Begum, N.Q. McDonald, A. Butler, D. Jones, K. Raine, C. Latimer, C.R. Santos, M. Nohadani, A.C. Eklund, B. Spencer-Dene, G. Clark, L. Pickering, G. Stamp, M. Gore, Z. Szallasi, J. Downward, P.A. Futreal, and C. Swanton. 2012. Intratumor heterogeneity and branched evolution revealed by multiregion sequencing. N.Engl.J.Med. 366:883-892.

Hanahan, D., and R.A. Weinberg. 2011. Hallmarks of cancer: the next generation. Cell. 144:646-674.

Hong, B.S., J.H. Cho, H. Kim, E.J. Choi, S. Rho, J. Kim, J.H. Kim, D.S. Choi, Y.K. Kim, D. Hwang, and Y.S. Gho. 2009. Colorectal cancer cell-derived microvesicles are enriched in cell cycle-related mRNAs that promote proliferation of endothelial cells. BMC Genomics. 10:556-2164-10-556.

How Kit, A., N. Mazaleyrat, A. Daunay, H.M. Nielsen, B. Terris, and J. Tost. 2013. Sensitive Detection of KRAS Mutations Using Enhanced-ice-COLD-PCR Mutation Enrichment and Direct Sequence Identification. Hum.Mutat. 34:1568-1580.

Huang, M., A. Shen, J. Ding, and M. Geng. 2014. Molecularly targeted cancer therapy: some lessons from the past decade. Trends Pharmacol.Sci. 35:41-50.

Jahr, S., H. Hentze, S. Englisch, D. Hardt, F.O. Fackelmayer, R.D. Hesch, and R. Knippers. 2001. DNA fragments in the blood plasma of cancer patients: quantitations and evidence for their origin from apoptotic and necrotic cells. Cancer Res. 61:1659-1665.

Jung, K., M. Fleischhacker, and A. Rabien. 2010. Cell-free DNA in the blood as a solid tumor biomarker--a critical appraisal of the literature. Clin.Chim.Acta. 411:1611-1624.

Kandoth, C., M.D. McLellan, F. Vandin, K. Ye, B. Niu, C. Lu, M. Xie, Q. Zhang, J.F. McMichael, M.A. Wyczalkowski, M.D. Leiserson, C.A. Miller, J.S. Welch, M.J. Walter, M.C. Wendl, T.J. Ley, R.K. Wilson, B.J. Raphael, and L. Ding. 2013. Mutational landscape and significance across 12 major cancer types. Nature. 502:333-339.

Karachaliou, N., C. Mayo, C. Costa, I. Magri, A. Gimenez-Capitan, M.A. Molina-Vila, and R. Rosell. 2013. KRAS mutations in lung cancer. Clin.Lung Cancer. 14:205-214.

Leary, R.J., M. Sausen, I. Kinde, N. Papadopoulos, J.D. Carpten, D. Craig, J. O'Shaughnessy, K.W. Kinzler, G. Parmigiani, B. Vogelstein, L.A. Diaz Jr, and V.E. Velculescu. 2012. Detection of chromosomal alterations in the circulation of cancer patients with whole-genome sequencing. Sci.Transl.Med. 4:162ra154.

Li, J., L. Wang, H. Mamon, M.H. Kulke, R. Berbeco, and G.M. Makrigiorgos. 2008. Replacing PCR with COLD-PCR enriches variant DNA sequences and redefines the sensitivity of genetic testing. Nat.Med. 14:579-584.

Lo, Y.M., J. Zhang, T.N. Leung, T.K. Lau, A.M. Chang, and N.M. Hjelm. 1999. Rapid clearance of fetal DNA from maternal plasma. Am.J.Hum.Genet. 64:218-224.

Lui, Y.Y., K.W. Chik, R.W. Chiu, C.Y. Ho, C.W. Lam, and Y.M. Lo. 2002. Predominant hematopoietic origin of cell-free DNA in plasma and serum after sex-mismatched bone marrow transplantation. Clin.Chem. 48:421-427.

Lui, Y.Y., K.W. Chik, and Y.M. Lo. 2002. Does centrifugation cause the ex vivo release of DNA from blood cells? Clin.Chem. 48:2074-2076.

Macher, H.C., M.A. Martinez-Broca, A. Rubio-Calvo, C. Leon-Garcia, M. Conde-Sanchez, A. Costa, E. Navarro, and J.M. Guerrero. 2012. Non-invasive prenatal diagnosis of multiple endocrine neoplasia type 2A using COLD-PCR combined with HRM genotyping analysis from maternal serum. PLoS One. 7:e51024.

Malmgren, J.A., J. Parikh, M.K. Atwood, and H.G. Kaplan. 2012. Impact of mammography detection on the course of breast cancer in women aged 40-49 years. Radiology. 262:797-806.

Mandel, P., and P. Metais. 1948. Les acides nucleiques du plasma sanguin chez l'homme. C.R.Seances Soc.Biol.Fil. 142:241-243.

McGrath, J.P., D.J. Capon, D.H. Smith, E.Y. Chen, P.H. Seeburg, D.V. Goeddel, and A.D. Levinson. 1983. Structure and organization of the human Ki-ras proto-oncogene and a related processed pseudogene. Nature. 304:501-506.

Misale, S., R. Yaeger, S. Hobor, E. Scala, M. Janakiraman, D. Liska, E. Valtorta, R. Schiavo, M. Buscarino, G. Siravegna, K. Bencardino, A. Cercek, C.T. Chen, S. Veronese, C. Zanon, A. Sartore-Bianchi, M. Gambacorta, M. Gallicchio, E. Vakiani, V. Boscaro, E. Medico, M. Weiser, S. Siena, F. Di Nicolantonio, D. Solit, and A. Bardelli. 2012. Emergence of KRAS mutations and acquired resistance to anti-EGFR therapy in colorectal cancer. Nature. 486:532-536.

Montagut, C., and J. Settleman. 2009. Targeting the RAF-MEK-ERK pathway in cancer therapy. Cancer Lett. 283:125-134.

Mouliere, F., B. Robert, E. Arnau Peyrotte, M. Del Rio, M. Ychou, F. Molina, C. Gongora, and A.R. Thierry. 2011. High fragmentation characterizes tumour-derived circulating DNA. PLoS One. 6:e23418.

NCCLS. Protocols for Determination of Limits of Detection and Limits of Quantitation; Approved Guideline. NCCLS document EP-17A [ISBN 1-56238-551-8]. NCCLS, 940 West Valley Road, Suite 1400, Wayne, Pennsylvania, 19087-1898 USA, 2004.

Nilsson, R.J., L. Balaj, E. Hulleman, S. van Rijn, D.M. Pegtel, M. Walraven, A. Widmark, W.R. Gerritsen, H.M. Verheul, W.P. Vandertop, D.P. Noske, J. Skog, and T. Wurdinger. 2011. Blood platelets contain tumor-derived RNA biomarkers. Blood. 118:3680-3683.

Oppenheim, D.E., R. Spreafico, A. Etuk, D. Malone, E. Amofah, C. Pena-Murillo, T. Murray, L. McLaughlin, B.S. Choi, S. Allan, A. Belousov, A. Passioukov, C. Gerdes, P. Umana, F. Farzaneh, and P. Ross. 2014. Glyco-engineered anti-EGFR mAb elicits ADCC by NK cells from colorectal cancer patients irrespective of chemotherapy. Br.J.Cancer. 110:1221-1227.

Owczarzy, R., Y. You, C.L. Groth, and A.V. Tataurov. 2011. Stability and mismatch discrimination of locked nucleic acid-DNA duplexes. Biochemistry. 50:9352-9367.

Park, J.L., H.J. Kim, B.Y. Choi, H.C. Lee, H.R. Jang, K.S. Song, S.M. Noh, S.Y. Kim, D.S. Han, and Y.S. Kim. 2012. Quantitative analysis of cell-free DNA in the plasma of gastric cancer patients. Oncol.Lett. 3:921-926.

Peters, D.L., and P.J. Pretorius. 2011. Origin, translocation and destination of extracellular occurring DNA--a new paradigm in genetic behaviour. Clin.Chim.Acta. 412:806-811.

Prior, I.A., P.D. Lewis, and C. Mattos. 2012. A comprehensive survey of Ras mutations in cancer. Cancer Res. 72:2457-2467.

Pupilli, C., P. Pinzani, F. Salvianti, B. Fibbi, M. Rossi, L. Petrone, G. Perigli, M.L. De Feo, V. Vezzosi, M. Pazzagli, C. Orlando, and G. Forti. 2013. Circulating BRAFV600E in the diagnosis and follow-up of differentiated papillary thyroid carcinoma. J.Clin.Endocrinol.Metab. 98:3359-3365.

Rak, J. 2013. Extracellular vesicles - biomarkers and effectors of the cellular interactome in cancer. Front.Pharmacol. 4:21.

Roberts, P.J., and C.J. Der. 2007. Targeting the Raf-MEK-ERK mitogen-activated protein kinase cascade for the treatment of cancer. Oncogene. 26:3291-3310.

Saltz, L.B., N.J. Meropol, S. Loehrer PJ, M.N. Needle, J. Kopit, and R.J. Mayer. 2004. Phase II trial of cetuximab in patients with refractory colorectal cancer that expresses the epidermal growth factor receptor. J.Clin.Oncol. 22:1201-1208.

Schulze, A., K. Lehmann, H.B. Jefferies, M. McMahon, and J. Downward. 2001. Analysis of the transcriptional program induced by Raf in epithelial cells. Genes Dev. 15:981-994.

Sequist, L.V., B.A. Waltman, D. Dias-Santagata, S. Digumarthy, A.B. Turke, P. Fidias, K. Bergethon, A.T. Shaw, S. Gettinger, A.K. Cosper, S. Akhavanfard, R.S. Heist, J. Temel, J.G. Christensen, J.C. Wain, T.J. Lynch, K. Vernovsky, E.J. Mark, M. Lanuti, A.J. Iafrate, M. Mino-Kenudson, and J.A. Engelman. 2011. Genotypic and histological evolution of lung cancers acquiring resistance to EGFR inhibitors. Sci.Transl.Med. 3:75ra26.

Shaukat, A., S.J. Mongin, M.S. Geisser, F.A. Lederle, J.H. Bond, J.S. Mandel, and T.R. Church. 2013. Long-term mortality after screening for colorectal cancer. N.Engl.J.Med. 369:1106-1114.

Skog, J., T. Wurdinger, S. van Rijn, D.H. Meijer, L. Gainche, M. Sena-Esteves, W.T. Curry Jr, B.S. Carter, A.M. Krichevsky, and X.O. Breakefield. 2008. Glioblastoma microvesicles transport RNA and proteins that promote tumour growth and provide diagnostic biomarkers. Nat.Cell Biol. 10:1470-1476.

Sozzi, G., D. Conte, L. Mariani, S. Lo Vullo, L. Roz, C. Lombardo, M.A. Pierotti, and L. Tavecchio. 2001. Analysis of circulating tumor DNA in plasma at diagnosis and during follow-up of lung cancer patients. Cancer Res. 61:4675-4678.

Taly, V., D. Pekin, L. Benhaim, S.K. Kotsopoulos, D. Le Corre, X. Li, I. Atochin, D.R. Link, A.D. Griffiths, K. Pallier, H. Blons, O. Bouche, B. Landi, J.B. Hutchison, and P. Laurent-Puig. 2013. Multiplex picodroplet digital PCR to detect KRAS mutations in circulating DNA from the plasma of colorectal cancer patients. Clin.Chem. 59:1722-1731.

Taniguchi, K., J. Uchida, K. Nishino, T. Kumagai, T. Okuyama, J. Okami, M. Higashiyama, K. Kodama, F. Imamura, and K. Kato. 2011. Quantitative detection of EGFR mutations in circulating tumor DNA derived from lung adenocarcinomas. Clin.Cancer Res. 17:7808-7815.

To, E.W., K.C. Chan, S.F. Leung, L.Y. Chan, K.F. To, A.T. Chan, P.J. Johnson, and Y.M. Lo. 2003. Rapid clearance of plasma Epstein-Barr virus DNA after surgical treatment of nasopharyngeal carcinoma. Clin.Cancer Res. 9:3254-3259.

Van Cutsem, E., C.H. Kohne, E. Hitre, J. Zaluski, C.R. Chang Chien, A. Makhson, G. D'Haens, T. Pinter, R. Lim, G. Bodoky, J.K. Roh, G. Folprecht, P. Ruff, C. Stroh, S. Tejpar, M. Schlichting, J. Nippgen, and P. Rougier. 2009. Cetuximab and chemotherapy as initial treatment for metastatic colorectal cancer. N.Engl.J.Med. 360:1408-1417.

Vaughn, C.P., S.D. Zobell, L.V. Furtado, C.L. Baker, and W.S. Samowitz. 2011. Frequency of KRAS, BRAF, and NRAS mutations in colorectal cancer. Genes Chromosomes Cancer. 50:307-312.

Vectibix® SmPC. Summary of Product Characteristics at http://www.medicines.org.uk/emc/medicine/20528. Updated on 28.05.2014. Retrieved on 05.01.2015.

Vogelstein, B., N. Papadopoulos, V.E. Velculescu, S. Zhou, L.A. Diaz Jr, and K.W. Kinzler. 2013. Cancer genome landscapes. Science. 339:1546-1558.

Wang, B.G., H.Y. Huang, Y.C. Chen, R.E. Bristow, K. Kassauei, C.C. Cheng, R. Roden, L.J. Sokoll, D.W. Chan, and I. Shih. 2003. Increased plasma DNA integrity in cancer patients. Cancer Res. 63:3966-3968.

Wang, M., T.M. Block, L. Steel, D.E. Brenner, and Y.H. Su. 2004. Preferential isolation of fragmented DNA enhances the detection of circulating mutated k-ras DNA. Clin.Chem. 50:211-213.

Wortzel, I., and R. Seger. 2011. The ERK Cascade: Distinct Functions within Various Subcellular Organelles. Genes Cancer. 2:195-209.

Ye, J., G. Coulouris, I. Zaretskaya, I. Cutcutache, S. Rozen, and T.L. Madden. 2012. Primer-BLAST: a tool to design target-specific primers for polymerase chain reaction. BMC Bioinformatics. 13:134-2105-13-134.

You, Y., B.G. Moreira, M.A. Behlke, and R. Owczarzy. 2006. Design of LNA probes that improve mismatch discrimination. Nucleic Acids Res. 34:e60.

Yu, J.L., L. May, V. Lhotak, S. Shahrzad, S. Shirasawa, J.I. Weitz, B.L. Coomber, N. Mackman, and J.W. Rak. 2005. Oncogenic events regulate tissue factor expression in colorectal cancer cells: implications for tumor progression and angiogenesis. Blood. 105:1734-1741.

Zhou, G.H., M. Gotou, T. Kajiyama, and H. Kambara. 2005. Multiplex SNP typing by bioluminometric assay coupled with terminator incorporation (BATI). Nucleic Acids Res. 33:e133.

Zuker, M. 2003. Mfold web server for nucleic acid folding and hybridization prediction. Nucleic Acids Res. 31:3406-3415.

Supplementary Table 1. Characteristics of the individual study participants.

| ID#	Age	Sex	Primary tumor	Treatment regimen	Tissue sample			Blood sample	cfDNA concentration / protocol (ng/ml)				Tumor burden (cm³)
					Type	Time of sampling	Mutation	Mutation	A	B	C	D	
1	56	F	rectum	irinotecan, oxaliplatin, bevacizumab	resection	2009	-	-	34.20	41.35	37.85	50.25	N/A
2	56	M	sigmoid	panitumumab	resection	2013	-	-	38.80	68.50	64.75	53.00	14.4
3	74	M	sigmoid	irinotecan, 5-FU, folinic acid, bevacizumab	resection	2009	p.G12S	-	64.25	64.00	63.75	63.00	7.3
4	71	F	rectum	irinotecan, 5-FU, folinic acid, bevacizumab	biopsy	2009	-	(c.35G>C) p.G12A	16.05	16.80	16.55	27.30	68.9
5	55	F	cecum	oxaliplatin, 5-FU, folinic acid	biopsy	2012	p.G13D	-	34.20	31.00	37.65	43.50	144.0
6	66	M	rectum	oxaliplatin, bevacizumab	biopsy (needle)	2011	p.G13D	(c.38G>A) p.G13D	69.25	62.75	60.50	57.75	2.6
7	64	M	ascending	irinotecan, 5-FU, bevacizumab	resection	2013	-	-	25.25	27.30	29.70	30.10	0.6
8	63	F	sigmoid	oxaliplatin, 5-FU, bevacizumab	resection	2013	p.G12V	-	11.30	19.50	20.20	21.95	6.9
9	79	F	cecum/sigmoid[1]	best palliative care[2]	resection	2011	-	-	159.75	172.75	185.00	186.75	224.6
10	65	M	cecum	oxaliplatin, panitumumab	N/A	2010	-	-	N/A	N/A	N/A	36.50	N/A
11	64	F	cecum	irinotecan, 5-FU, bevacizumab	resection	2010	p.G12V	-	28.50	31.15	N/A	40.00	3.9
12	63	F	descending	oxaliplatin, 5-FU	resection	2009	(p.Q61H)	-	171.25	185.00	178.50	166.00	43.3
13	83	F	rectum	irinotecan, 5-FU, folinic acid, bevacizumab	resection	2010	p.G12D	-	33.90	26.85	39.35	38.20	N/A
14	60	M	rectum	oxaliplatin, capecitabine, panitumumab	biopsy	2013	-	-	23.35	28.45	27.50	30.75	13.4
15	63	F	sigmoid	irinotecan, 5-FU, folinic acid	resection	2012	-	-	51.25	55.25	53.00	55.50	9.4
16	57	M	cecum	oxaliplatin, 5-FU, folinic acid, bevacizumab	N/A	2008	-	-	46.00	53.00	46.85	51.75	64.8

5-FU = fluorouracil

[1] Synchronous tumors

[2] Preceded by panitumumab and simultaneous disease progression.
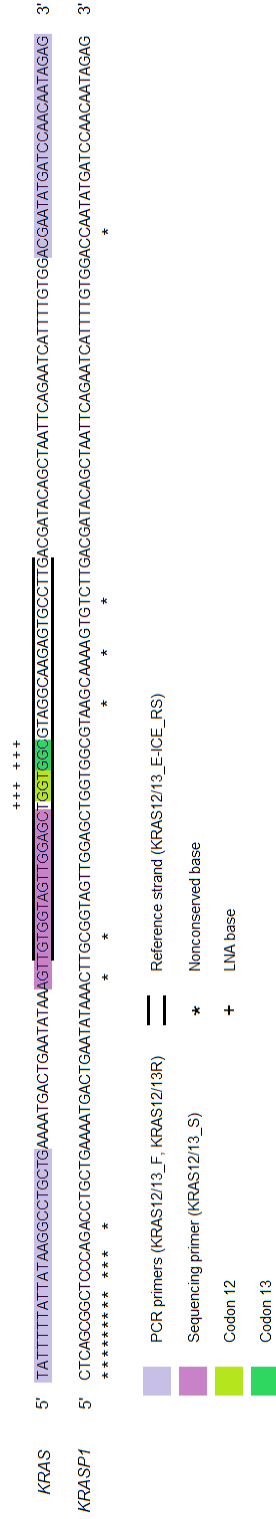
Supplementary Figure 1. Oligonucleotides used in the E-ice-COLD-PCR-enhanced targeted pyrosequencing assay and their relation to *KRAS* and *KRASP1* (pseudogene).
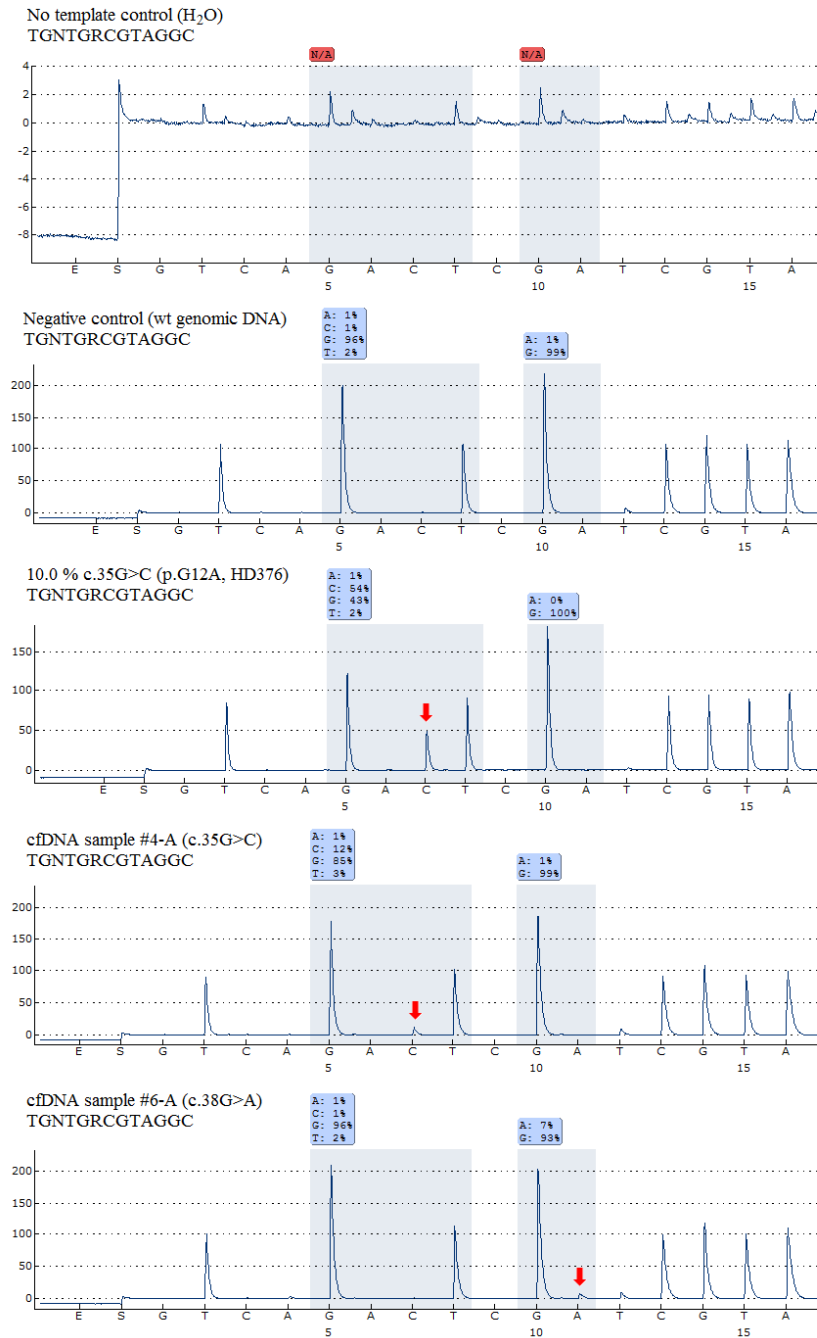
Supplementary Figure 2. Some examples of the pyrosequencing data. Red arrows denote actual base alterations, while percentages refer to the total signal output of the 35th and 38th base in each sequence (N and R, respectively).